



Department of Energy
Office of Civilian Radioactive Waste Management
Yucca Mountain Site Characterization Office
P.O. Box 30307
North Las Vegas, NV 89036-0307

QA: N/A

MAR 12 2001

OVERNIGHT MAIL

C. William Reamer, Chief
High-Level Waste and Performance
Assessment Branch
Division of Waste Management
Office of Nuclear Materials Safety
and Safeguards
U.S. Nuclear Regulatory Commission
Two White Flint North
Rockville, MD 20852

RESPONSES TO RADIONUCLIDE TRANSPORT KEY TECHNICAL ISSUE TECHNICAL EXCHANGE: SUBISSUE 3, AGREEMENT 6; AND STRUCTURAL DEFORMATION AND SEISMICITY KEY TECHNICAL ISSUE TECHNICAL EXCHANGE: SUBISSUE 3, AGREEMENT 2

The subject agreements asked the U.S. Department of Energy to document the pre-test predictions for the Alcove 8-Niche 3 work. The enclosure to this letter contains the pre-test predictions for the Alcove 8-Niche 3 Phase 1 tests. A draft copy of the enclosure was provided to the U.S. Nuclear Regulatory Commission (NRC) Onsite Representative on February 23, 2001.

The enclosure contains the Phase I pre-test predictions for the flow and transport tests in the large plot and the tracer transport tests in the small plot test. Attachment II of the enclosure contains flow predictions for the small plot test. The enclosure also contains, as Attachment I, the Alcove 8-Niche 3 Cross-Over Test Plan, Revision 01. The revised test plan incorporates NRC's comments.

This transmittal constitutes a complete response to the subject agreements. If you have any questions relative to this letter and enclosure, please contact Timothy C. Gunter at (702) 794-1343 or Eric T. Smistad at (702) 794-5073.

Stephan Brocoum
Assistant Manager, Office of
Licensing and Regulatory Compliance

OL&RC:TCG-0832

Enclosure:
Pre-Test Predictions for Alcove 8-Niche 3
Crossover Test w/attachments

NIMSS20

MAR 12 2001

cc w/encl:

K. C. Chang, NRC, Rockville, MD
J. W. Anderson, NRC, Rockville, MD
D. J. Brooks, NRC, Rockville, MD
J. W. Bradbury, NRC, Rockville, MD
C. J. Glenn, NRC, Las Vegas, NV
S. H. Hanauer, DOE/HQ (RW-2) Las Vegas, NV
B. J. Garrick, ACNW, Rockville, DC
Richard Major, ACNW, Washington, DC
W. D. Barnard, NWTRB, Arlington, VA
Budhi Sagar, CNWRA, San Antonio, TX
W. C. Patrick, CNWRA, San Antonio, TX
Steve Kraft, NEI, Washington, DC
J. H. Kessler, EPRI, Palo Alto, CA
F. S. Echols, Winston & Strawn, Washington, DC
J. R. Curtiss, Winston & Strawn, Washington, DC
R. R. Loux, State of Nevada, Carson City, NV
Alan Kalt, Churchill County, Fallon, NV
D. A. Bechtel, Clark County, Las Vegas, NV
Harriet Ealey, Esmeralda County, Goldfield, NV
Leonard Fiorenzi, Eureka County, Eureka, NV
Andrew Remus, Inyo County, Independence, CA
Mickey Yarbrow, Lander County, Battle Mountain, NV
Jason Pitts, Lincoln County, Caliente, NV
L. W. Bradshaw, Nye County, Pahrump, NV
John Meder, State of Nevada, Carson City, NV
Michael King, Inyo County, Edmonds, WA
Judy Shankle, Mineral County, Hawthorne, NV
Jerry McKnight, Nye County, Tonopah, NV
Josie Larson, White Pine County, Ely, NV
R. I. Holden, National Congress of American
Indians, Washington, DC
Allen Ambler, Nevada Indian Environmental
Coalition, Fallon, NV

cc w/o encl:

N. K. Stablein, NRC, Rockville, MD
S. L. Wastler, NRC, Rockville, MD
W. L. Belke, NRC, Las Vegas, NV
L. H. Barrett, DOE/HQ (RW-1) FORS
A. B. Brownstein, DOE/HQ (RW-52) FORS
R. A. Milner, DOE/HQ (RW-2) FORS
N. H. Slater, DOE/HQ (RW-52) FORS
Nancy Williams, BSC, Las Vegas, NV
L. J. Trautner, BSC, Las Vegas, NV
R. S. Hajner, BSC, Las Vegas, NV
S. J. Cereghino, BSC, Las Vegas, NV

MAR 12 2001

cc w/o encl: (continued)

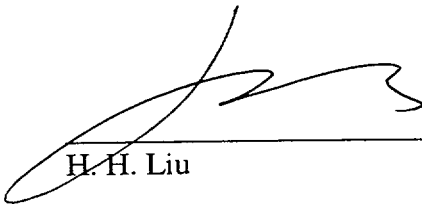
R. W. Andrews, BSC, Las Vegas, NV
Donald Beckman, BSC, Las Vegas, NV
G. D. Gardner, BSC, Las Vegas, NV
K. R. Iyengar, BSC, Las Vegas, NV
George Pannell, BSC, Las Vegas, NV
L. T. Skoblar, BSC, Las Vegas, NV
J. G. Linhart, BSC/NSNFP, Las Vegas, NV
J. H. Smyder, BSC/NSNFP, Las Vegas, NV
R. B. Bradbury, MTS, Las Vegas, NV
K. M. Cline, MTS, Las Vegas, NV
J. R. Dyer, DOE/YMSCO, Las Vegas, NV
D. G. Horton, DOE/YMSCO, Las Vegas, NV
Stephan Brocoum, DOE/YMSCO, Las Vegas, NV
D. R. Williams, DOE/YMSCO, Las Vegas, NV
A. V. Gil, DOE/YMSCO, Las Vegas, NV
S. P. Mellington, DOE/YMSCO, Las Vegas, NV
J. M. Replogle, DOE/YMSCO, Las Vegas, NV
E. T. Smistad, DOE/YMSCO, Las Vegas, NV
T. C. Gunter, DOE/YMSCO, Las Vegas, NV
D. L. Barr, DOE/YMSCO, Las Vegas, NV
C. L. Hanlon, DOE/YMSCO, Las Vegas, NV
S. A. Morris, DOE/YMSCO, Las Vegas, NV
P. G. Harrington, DOE/YMSCO, Las Vegas, NV
J. T. Sullivan, DOE/YMSCO, Las Vegas, NV
C. A. Kouts, DOE/YMSCO (RW-2) FORS
OL&RC Library
Records Processing Center =
(ENCL = READILY AVAILABLE)

Bechtel SAIC Company, LLC

Pre-Test Predictions for Alcove 8 -Niche 3 Cross-Over Test

February 2001

Prepared by:



H. H. Liu

2-27-01
Date

Approved by:



G.S. Bodvarsson
UZ Department Manager

2/27/01
Date

ENCLOSURE

Pre-Test Predictions for Alcove 8 –Niche 3 Cross-Over Test

1. Introduction

Infiltration and tracer tests are planned at the cross-over test site where Alcove 8 in the Enhanced Characterization of Repository Block (ECRB) Cross Drift is about 20 m directly above Niche 3 in the Exploratory Studies Facility (ESF) Main Drift. The major test objectives are: 1. quantification of large-scale (~20 m) infiltration and seepage processes in the potential repository horizon, 2. estimation of relations between relative permeability and water potential for unsaturated flow in faults and fracture networks, and 3. evaluation of the importance of matrix diffusion in the unsaturated zone (UZ) transport processes. This report addresses DOE/NRC Radionuclide Transport Technical Exchange Subissue 3, Agreement 6 (CRWMS M&O 2001).

The planned tests consist of several phases (see Attachment I). This report only provides predictions for Phase I. In each phase, liquid (with or without tracers) is released from infiltration plots at Alcove 8 and detected at Niche 3. In Phase I, a water pressure head of 2 cm will be kept at the infiltration plots, while infiltration rate will be reduced step by step in the other phases. In addition to practical considerations for performing the tests, use of this test condition for Phase I allows matrix blocks near fracture-matrix interfaces within flow paths to have relatively high saturation. Because of this, matrix imbibition is considerably reduced in the later stage of Phase I and other phases of the tests. Significant matrix imbibition would make evaluating the importance of matrix diffusion difficult. On the other hand, it is important to note that infiltration rates in the other phases are planned to be fractions of the infiltration rate in Phase I. Therefore, Phase I tests provide baseline information for important test parameters (e.g., infiltration rate) to be used in the other phases.

The Alcove 8-Niche 3 cross-over tests will be conducted in two locations (see Attachment I) at Alcove 8 using the same test procedure at each location. They correspond to small and large infiltration plots. The small plot is associated with a nearly vertical fault. Preliminary modeling studies have been performed to predict the test

results for Phase I. Whereas the modeling results for infiltration/seepage process were previously reported for the small plot test (see Attachment II), this report describes the modeling results for the large plot test and the tracer transport results for the small plot test as well. Since the test parameters (such as infiltration rate) to be used in other phases are related to test results from Phase I, model predictions of the test results for the other phases will be provided after values for these test parameters become available.

2. Modeling Approach and Rock Properties

Considering that model calibration, which involves many forward simulation runs, will be used to match the test results in the future, a relatively simple, cylindrical numerical grid is used for the large infiltration plot test (Figure 1). The grid extends about 25 m in the vertical direction and about 33 m in the radial direction (the diameter is about 66 m). The model domain is considered to be large enough, in comparison with size of the niche and the infiltration application area, such that side boundaries have insignificant effects on flow and transport near the alcove. The fine grid is used around the niche and relatively coarse grid away from it. To capture the transient behavior for flow between fractures and the matrix, the MINC (Multiple Interacting Continua) (Pruess and Narasimhan 1985) with five matrix continua was employed. In this study, ITOUGH2 code (Finsterie 1997) is used for modeling infiltration/seepage processes and T2R3D code (Wu et al. 1996) for modeling the tracer transport.

A constant pressure head (2 cm) is imposed on the top boundary corresponding to the infiltration plot, while a zero-flow condition in the vertical direction is used for the rest of the top boundary. (Ambient percolation flux is expected to be insignificant compared with the infiltration rates from the infiltration plot.) The side boundary corresponds to a zero-flow condition in the radial direction, with niche wall modeled by a zero capillary-pressure condition, representing a relative humidity of 100% in the niche. The bottom boundary condition is approximated by a free drainage condition. Initially, matrix saturations within the model domain are assumed to be the average ones under ambient conditions (given in Table 1) (Flint 1998). A small fracture saturation of 1.05% is assumed as the initial condition for fractures.

The drift-scale property set (Table 1) is employed in this modeling study (CRWMS M&O 2000a; CRWMS M&O 2000b). Because of the scale of the problem, the drift-scale properties are considered to be more suitable than the mountain-scale ones (CRWMS M&O 2000a). Fracture permeability values measured with disk infiltrometer by USGS are also consistent with the drift-scale fracture permeability values.

3. Sensitivity Study Results

A sensitivity study was first performed to identify key rock properties that would determine the experimental observations and to evaluate effects of rock property uncertainty on model prediction. The study results are presented in Figures 2-7. In each of these figures, only one rock property (for both TSw34 and TSw33) varies from those given in the drift-scale property set, while other parameters are held constant. The recoverability in these figures is defined as the total volume of water collected at Niche 3 divided by the total volume of water applied from the infiltration plot.

Model prediction results are not sensitive to the active fracture model parameter γ (Figure 2). Under the test conditions for Phase I, fracture saturation in a flow path is close to 100%, which results in similar constitutive relations in the fracture continuum for a range of γ values (Liu et al. 1999). Model prediction results are very sensitive to fracture permeability (Figure 3). Higher fracture permeability corresponds to an earlier wetting front arrival time for the modeled test period. The fracture alpha also has a significant effect on the arrival time and the recoverability because smaller fracture alpha gives rises to a strong capillary barrier effect (Figure 4). Compared with fracture permeability and alpha, fracture porosity, matrix permeability and matrix alpha have relatively insignificant effects on the wetting front arrival time and recoverability (Figures 5 to 7). These results are generally consistent with the sensitivity study results for the small infiltration plot test (Liu 2000).

4. Model Prediction of Water Arrival Time and Recoverability

The sensitivity study results indicated that the water arrival time and recoverability to be observed at Niche 3 are mainly controlled by fracture permeability and alpha. Figure 8 shows model prediction results for the drift-scale property set, increased fracture permeability and reduced fracture permeability. The increased and reduced fracture permeabilities are given by $20K_f^*$ and $K_f^*/20$, respectively, where K_f^* is fracture permeability given in Table 1. They roughly correspond to $K_f^* \times 10^{2\sigma}$ and $K_f^* \times 10^{-2\sigma}$, respectively, where σ is the standard deviation of $\log(kf)$ for tsw34 (DTN: LB990501233129). The fracture alpha is related to fracture permeability with the well-known Miller-Miller similarity (Miller and Miller 1956). Times for the seepage to first occur are 0.85 ($K_f = K_f^*$), 0.02 ($K_f = 20K_f^*$) and 63.8 ($K_f = K_f^*/20$) days for the three property sets. In general, the property sets with increased and reduced fracture permeabilities are expected to correspond to lower and upper limits of the water arrival time.

Figure 9 shows predicted relations between the water arrival time and infiltration rate from the large infiltration plot, to allow for the effects of property uncertainty. The infiltration rate is approximately proportional to fracture permeability. Because the infiltration rate can be easily measured before the wetting front is observed at Niche 3, this figure is useful for *in situ* prediction of the arrival time based on the observed infiltration rate. For the curve in Figure 9, rock property values are fixed except for fracture permeability and fracture alpha that are correlated based on the Miller-Miller similarity. To demonstrate the usefulness of Figure 9, assume that the infiltration rate is 650 L/day. In this case, predicted arrival time is about 20 days, as shown in Figure 9.

5. Evaluation of the Effect on Rock Hydrologic Conditions for the Potential Waste Package Closest to the Test Site

One concern about the cross-over test is its possible effect on rock hydrologic conditions around potential waste packages close to the test site. To evaluate this potential effect, a modeling analysis was performed based on the following conservative assumption. According to the current test plan (see Attachment I), the test will start with a 2 cm

pressure head at the infiltration plot. Then, the pressure will decrease such that the infiltration rate will be reduced step by step. To be conservative, it was assumed in the modeling analysis that a 2 cm pressure head will be kept during the entire test period. Since use of the increased permeabilities gives a very short water arrival time (0.02 days), these permeabilities are not used for modeling studies in this section. Length of test period depends on the infiltration rate and fracture permeability. Under the current test plan (see Attachment I), the test period is expected to be less than 1 year for the drift-scale property set. In flow predictions for the small infiltration plot tests (see Attachment II), it was found that the size of infiltrating water plume is smaller for the reduced fracture permeability than that for the drift-scale property set. Therefore, the case corresponding to the reduced fracture permeability can be conservatively neglected.

Figure 10 shows predicted distributions of matrix saturation increase as a result of the test, both (a) at the end of the test (1 year) and (b) at 10 years. The matrix saturation increase is determined to be the difference between predicted matrix saturations with and without consideration of the test. These results suggest that the test does not significantly affect rock hydrologic conditions for a location about 10 m away from the niche center (in the horizontal direction). The horizontal distance between the drift containing the closest potential waste package and the test location is about 30 m. Therefore, predictions for this conservative scenario indicate that this test will not affect rock hydrologic conditions around the drift containing potential waste package close to the test site.

6. Implications for Test Design

From the mass-balance point of view, uncertainties in the indirect estimates of water moving around the niche will lead to uncertain estimates of water diversion. NRC staff and YMP scientists have suggested that the diverted water can be more directly measured by cutting slots along the walls of Niche 3. These slots would be about 1 meter deep and angled upward from the niche walls. The purpose of the 1 m slot would be to estimate the amount of water diverted around the drift as a result of the capillary barrier effect associated with the niche opening.

The tuff interface could spread the plumes and potentially promote lateral flows. The preliminary model results as illustrated in Figure 10 suggest that large amount of water bypasses the niche by lateral spreading at the lithophysal-nonlithophysal interface. The slots needed to be much deeper than 1 meter to capture both the diverted flow and the bypassed flow. It will be a great technical challenge to excavate 10 m deep slots around the niche walls, with supports carefully planned to preserve the integrity of the slots and to minimize the perturbations to the host rocks above the slots.

The current plan calls for the continuance of model updates against liquid-release tests at least through the fault test periods. The wetting-front detection arrays from Niche 3 boreholes and the geophysical tomographic images will be used to provide direct and indirect information to delineate the plumes for the relatively small releases. The slot excavation techniques need to be further evaluated at other test beds before large-scale deployments at the Alcove 8 - Niche 3 site.

The seepage diversion can be more effectively evaluated with a slot at Niche 5 in lieu of the crossover test bed with a lithophysal-nonlithophysal interface. The slot for a mass-balance approach has been used in the Alcove 6 fracture-matrix test bed to interpret the series of liquid-release tests above a slot. The Alcove 6 experience in middle nonlithophysal tuff can be applied to Niche 5 in the lower lithophysal tuff. Niche 5 is located near the center of the potential repository block, 1,620 m along the Cross Drift in a location with high cavity density. The lower lithophysal tuff is the main potential repository unit, where 78% of the potential waste-emplacement drifts are located. Niche 5 has both horizontal and slanted boreholes above the niche ceiling for controlled releases at different distances to the niche ceiling. Seepage diversion studies can be more efficiently planned with diversions of liquid releases more likely to be captured by inclined slots if diversions occur primarily along narrow zones around the niche openings.

The niche test sites are designed for localized releases above the niche ceiling to quantify the seepage thresholds. The seepage-diversion quantification is important in the niche

tests, as recognized by the NRC Staff, the Drift Seepage Peer Review Panel, and the YMP scientists. All liquid tests have concerns about uncertainties associated not only with seepage diversion but also with the loss due to evaporation and storage, resulting from matrix imbibition and in secondary fractures.

Figure 11 illustrates the test beds at Niche 5, with potential additions of upward-angled slots around the end of the niche and other test components along the access drift. The test plan at Niche 5 is still evolving, following the same process of plan development at Alcove 8-Niche 3. Site-specific models, flexible testing approaches with contingencies, and continuing technology evaluation of excavation and testing techniques, are the basis for developing practical plans, evaluating critical processes, and assessing the potential impact on the potential repository performance. The Niche 5 test plans, together with the slot excavation evaluations, are in progress.

7. Model Prediction of Tracer Breakthrough Curves at Niche 3

At the late stage of Phase I, two tracers (Br and PFBA (pentafluorobenzoic acid) with molecular diffusion coefficient values of 2.08×10^{-9} and 7.6×10^{-10} m²/s, respectively) will be introduced into the infiltrating water from infiltration plots at Alcove 8. The major objective of tracer tests is to demonstrate the importance of matrix diffusion.

Figure 12 shows predicted breakthrough curves for the large infiltration plot using three property sets (drift-scale property set, increased fracture permeability and reduced fracture permeability). The predicted breakthrough curves for the small infiltration plot are also shown in Figure 13. Details for modeling results of water flow for the small infiltration plot can be found in Liu (2000). In the tracer transport predictions for the property set with increased fracture permeability, tracers are assumed to be introduced one day after water arrival at Niche 3. For the rock property set with reduced fracture permeability and drift-scale property set, tracers are assumed to be introduced ten days after water arrival at Niche 3. In Figures 12 and 13, zero time corresponds to the time when tracers are introduced into infiltrating water.

The previous modeling study on Alcove 1 test showed that the dispersion process in fractures has an insignificant effect on tracer transport behavior. On the other hand, as a result of low water flow velocity in the matrix, the mechanical dispersion in the matrix can be ignored. Consequently, dispersivity values for the fracture and matrix continua are set to zero in the tracer transport predictions. Tortuosity values for matrix diffusion are calculated using the classic formulation given by Millington and Quirk (1961). Considering that matrix water saturation is close to 100% near a fracture-matrix interface when tracers are introduced, 100% matrix saturation was assumed for calculating the tortuosity values (0.54 for Tsw33 and 0.48 for Tsw34).

As shown in Figures 12 and 13, Br breaks through later than PFBA because Br has a larger molecular diffusion coefficient. Therefore, it is expected that the importance of the matrix diffusion may be noticed in Phase I. It is also expected that the importance of matrix diffusion will be more noticeable in the other phases because the degree of matrix diffusion depends on the residence time of infiltrating water with tracers in the rock formation. In general, breakthrough curves are expected to be bounded by modeling results, based on property sets with increased and reduced fracture permeabilities.

Note that some factors that may considerably affect observed breakthrough curves are not considered in these predictions. For example, both tracers are considered to be conservative because some sorption may occur in the tests as a result of fracture coatings. On the other hand, small fractures with trace length less than 0.3 m are not considered in the predictions. These small fractures result in a larger fracture-matrix interface area than used in the predictions and therefore enhance the matrix diffusion. These factors will be considered in future comparison between predicted and observed breakthrough curves.

8. Summary and Conclusions

1. Model prediction indicates that for the large infiltration plot test, the likely wetting front arrival time at Niche 3 ranges from less than one day to about two months. Considering the rock property uncertainties, a predicted relation between the potential arrival time and the infiltration rate is provided as a tool for *in situ* prediction of the arrival time, based on the actual infiltration rate.
2. Predicted water arrival time and recoverability are sensitive to fracture permeability and alpha for the large infiltration plot test.
3. A conservative scenario indicates that the large infiltration plot test will not affect rock hydrologic conditions around the potential water package close to the test site.
4. Predicted tracer breakthrough curves for both large and small plot tests indicate that the effects of matrix diffusion may be noticeable in Phase I. It is also expected that the effects will be more noticeable in the other phases of Alcove 8-Niche 3 tests.
5. Because test parameter values to be used in the other phases of the tests are determined by observations from Phase I, this report only describes predictions for Phase I.
6. Water flowing from Alcove 8 to Niche 3 spreads up to 10 meters laterally, primarily due to contrasts in rock properties at the a lithophysal-nolithophysal interface. This results in a requirement for extremely deep slots (about 10 m deep) at Niche 3 to perform the seepage diversion test. Therefore, seepage diversion can be more effectively performed with a slot at Niche 5 in lieu of the crossover test bed.

References

- CRWMS M&O 2000a. *Analysis of Hydrologic Properties Data*. ANL-NBS-HS-000002 REV 00. Las Vegas, Nevada: CRWMS M&O. MOL.19990721.0519.
- CRWMS M&O 2000b. *Calibrated Properties Model*. MDL-NBS-HS-000003 REV 00. Las Vegas, Nevada: CRWMS M&O. MOL.19990721.0520.
- CRWMS M&O 2001. Summary Highlights of NRC/DOE Technical Exchange on Radionuclide Transport KTI, December 5 to December 7, 2000 - Berkeley, California. Las Vegas, Nevada: CRWMS M&O. MOL. 20010117.0063.
- Finsterle, S. 1997, ITOUGH2 Command Reference, Version 3.1, Rep. LBNL-40041, Lawrence Berkeley National Laboratory, Berkeley, CA.
- Flint, L.E. 1998, Characterization of hydrologic units using matrix properties, Yucca Mountain, Nevada, USGS Water Resources Investigation Report 97-4243.
- Liu, H.H., C. Doughty and G.S. Bodvarsson, An active fracture model for unsaturated flow and transport in fractured rocks, *Water Resour. Res.*, 34(10), 2633-2646,1998.
- Miller, E.E. and R.D. Miller, 1956, Physical theory for capillary flow phenomena, *J. Appl. Phys.* 27, 324-332.
- Millington, R.J. and J.M. Quirk 1961, Permeability of porous solids, *Trans. Faraday Soc.*, 57, 1200-1207.
- Pruess, K. and T.N. Narasimhan 1985, A practical method for modeling fluid and heat flow in fractured porous media, *Soc. Pet. Eng. J.* 25(1), 14-16.
- Wu, Y.S., C.F. Ahlers, P. Fraser, A. Simmons and K. Pruess 1996, Software qualification of selected TOUGH2 modules, LBNL-39490, Lawrence Berkeley National Laboratory, Berkeley, CA.

Table 1. Rock Properties Used in the Model Prediction for the Large Infiltration Plot Test

Rock property	TSw33		TSw34	
	Fracture	Matrix	Fracture	Matrix
Permeability (m ²)	5.5E-13	3.08E-17	2.76E-13	4.07E-18
Porosity	6.6E-3	0.154	1.E-2	0.11
Fracture spacing (m)	1.23		0.23	
Gamma	0.41		0.41	
Van Genuchten alpha (Pa ⁻¹)	1.46E-3	2.13E-5	5.16E-4	3.86E-6
Van Genuchten m	0.608	0.298	0.608	0.291
Residual saturation	0.01	0.12	0.01	0.19
Initial saturation	1.05E-2	0.72	1.05E-2	0.85

Figure 1. Numerical Grid for Model Prediction of Large Infiltration Plot Test

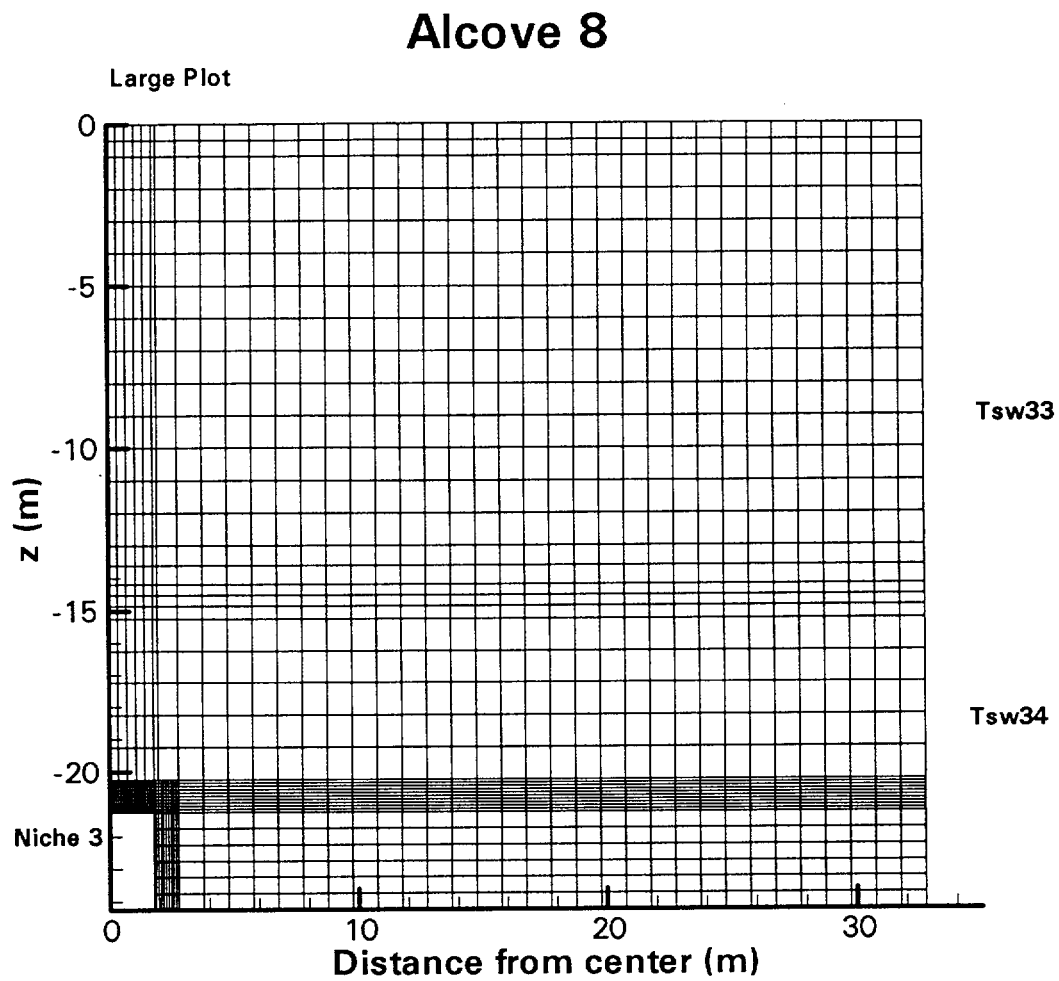


Figure 2. Simulation Results for Different Gamma Values.

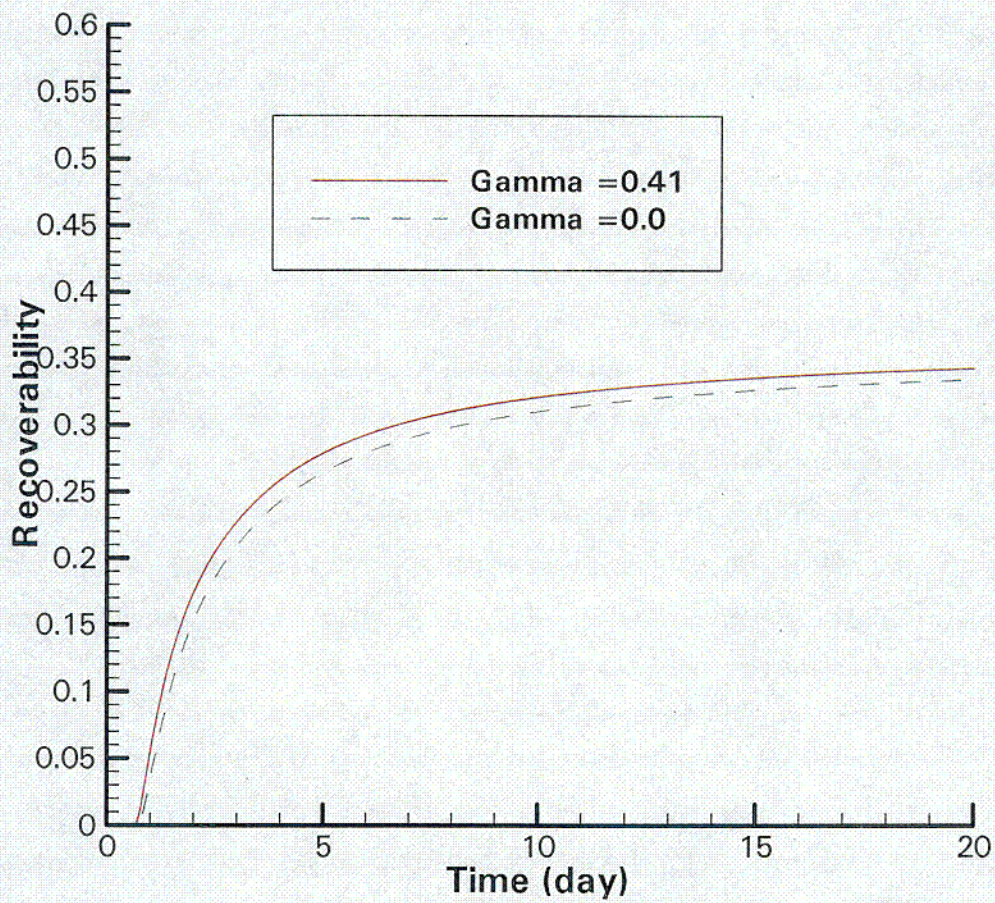


Figure 3. Simulation Results for Different Fracture Permeabilities (kf)

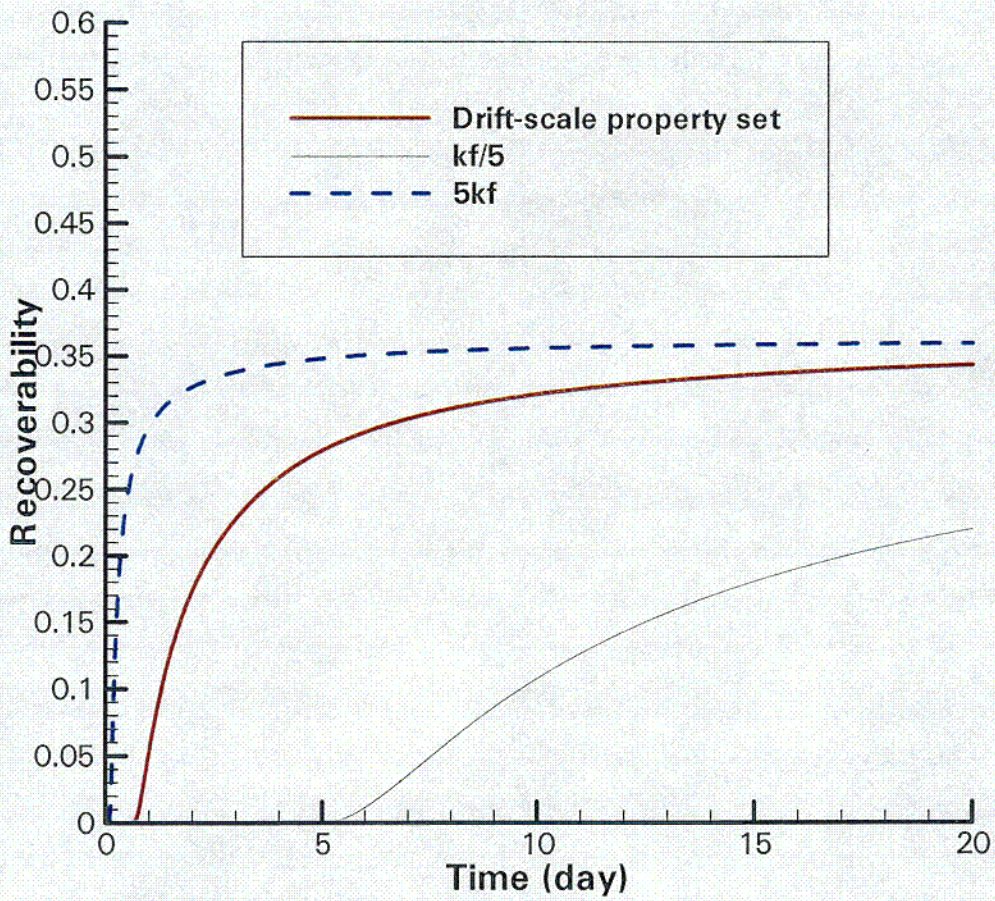


Figure 4. Simulation Results for Different Fracture Alphas

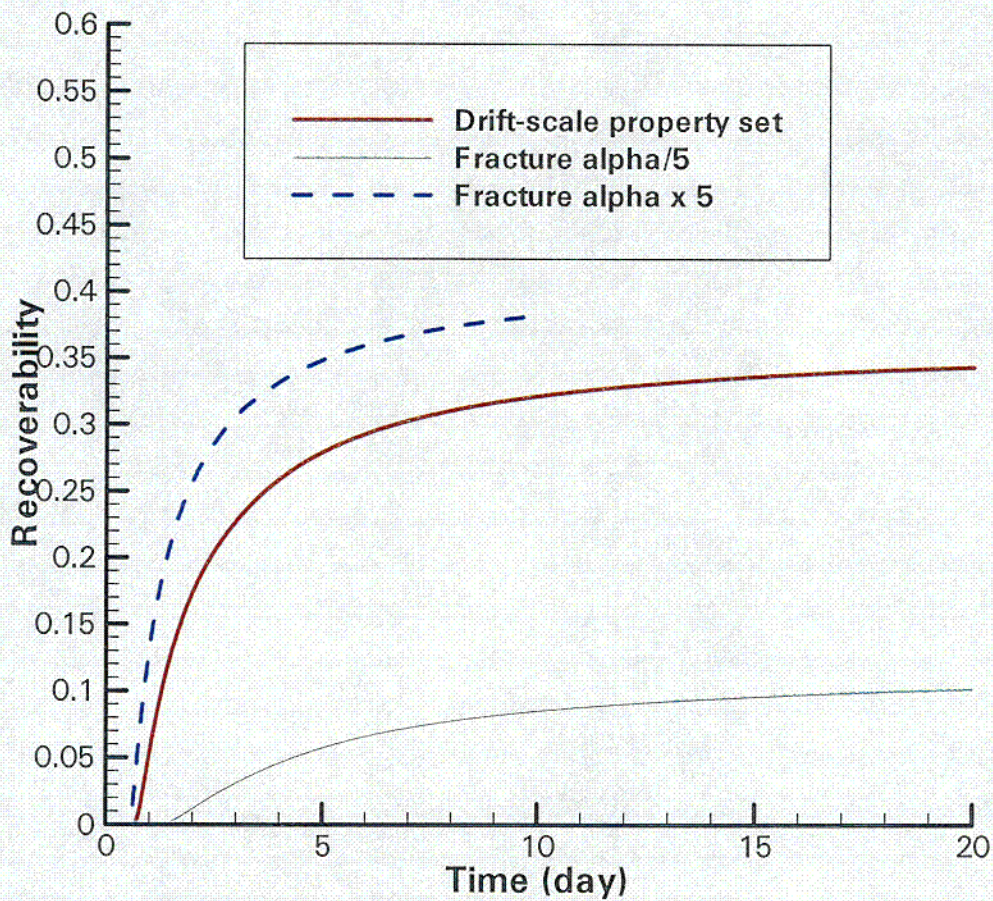


Figure 5. Simulation Results for Different Fracture Porosities

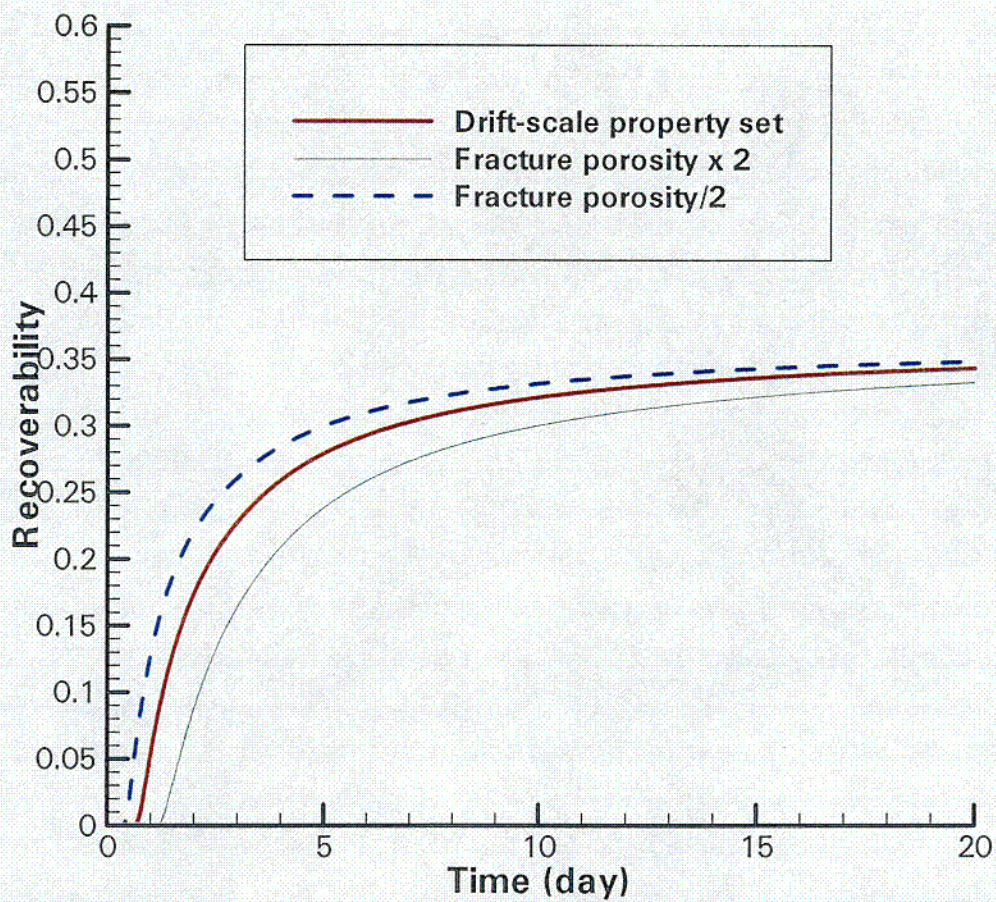


Figure 6. Simulation Results for Different Matrix Permeabilities (Km)

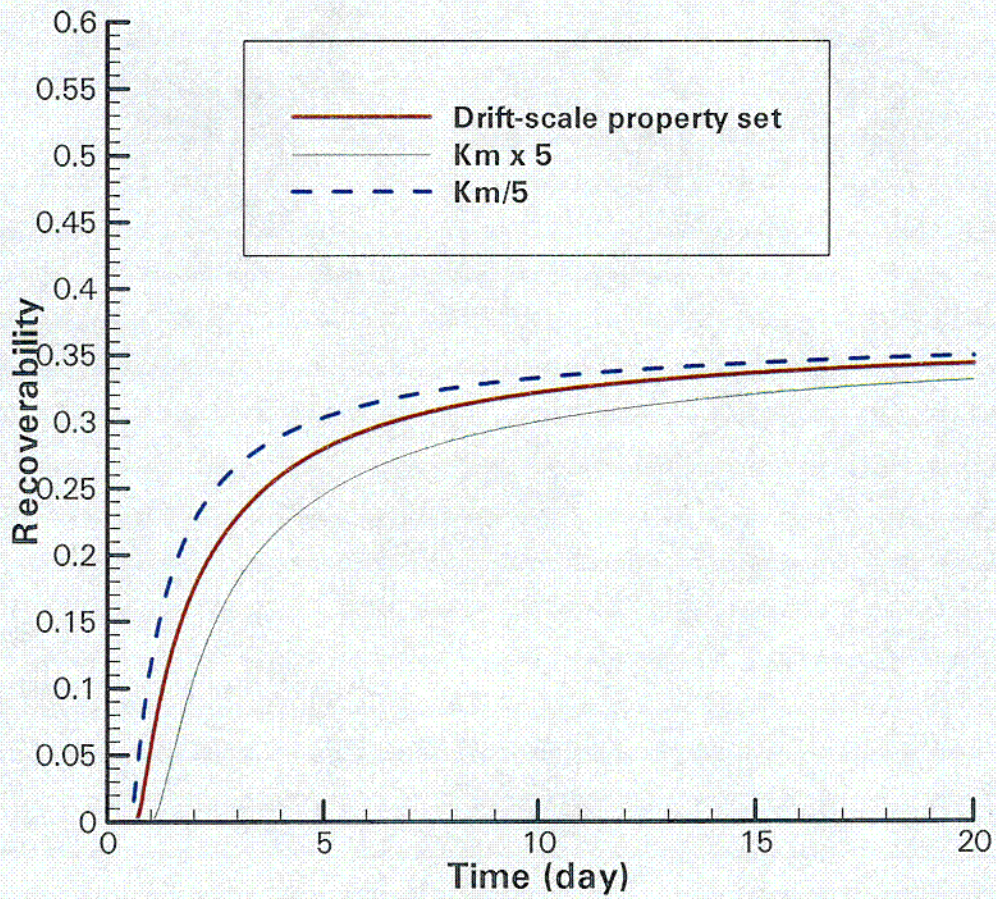


Figure 7 Simulation Results for Different Matrix Alphas

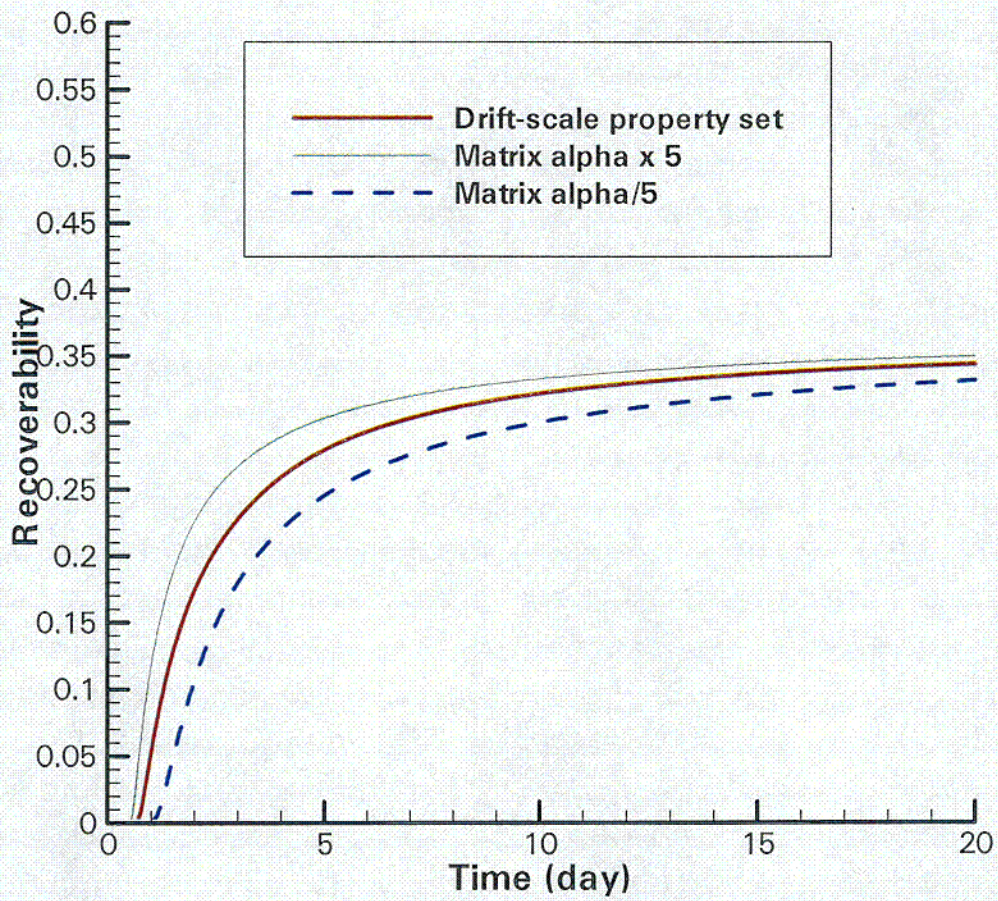


Figure 8. Predicted Recoverabilities for the Drift-Scale Property Set, Increased Fracture Permeability and Reduced Fracture Permeability.

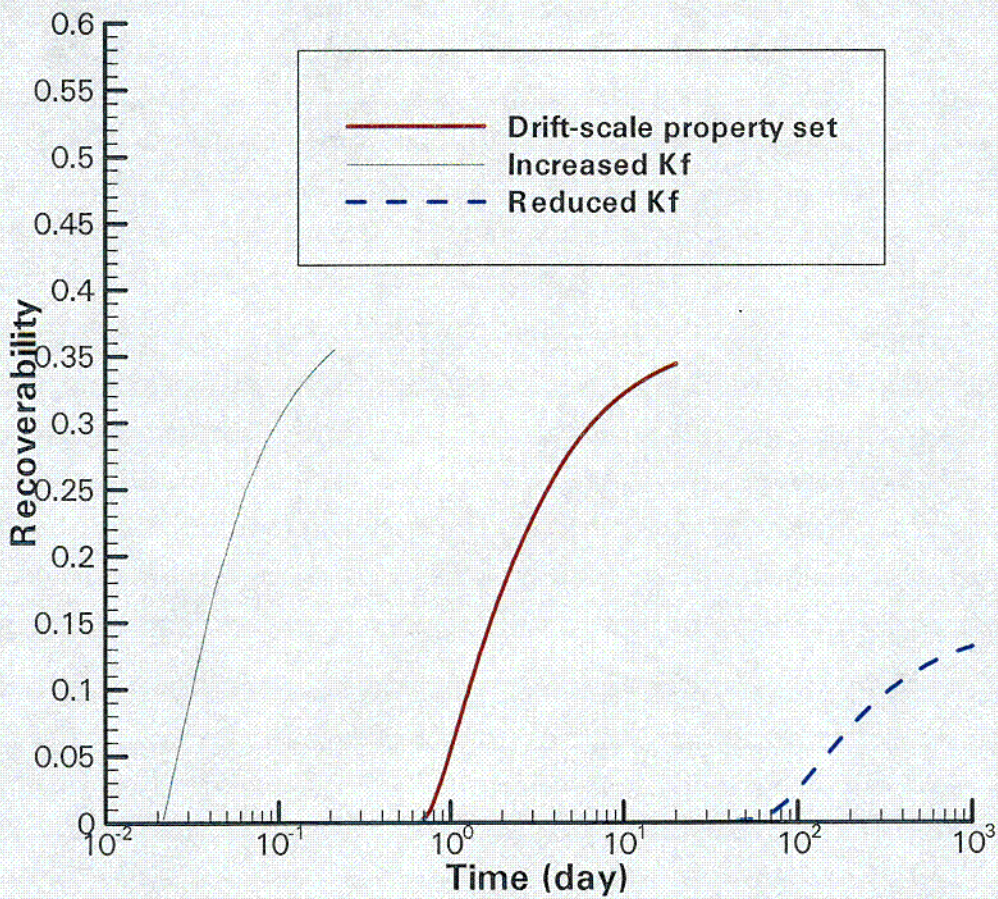


Figure 9. Simulated Relations between the Wetting Front Arrival Time and the Infiltration Rate of the Large Plot.

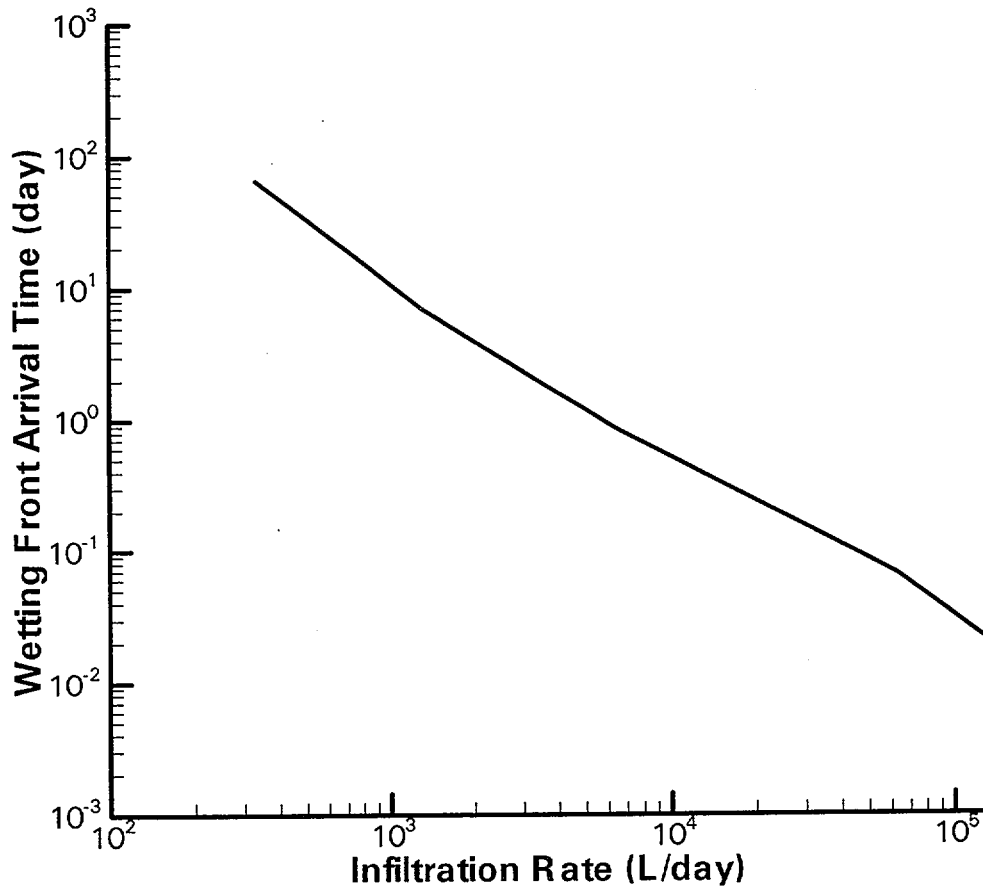
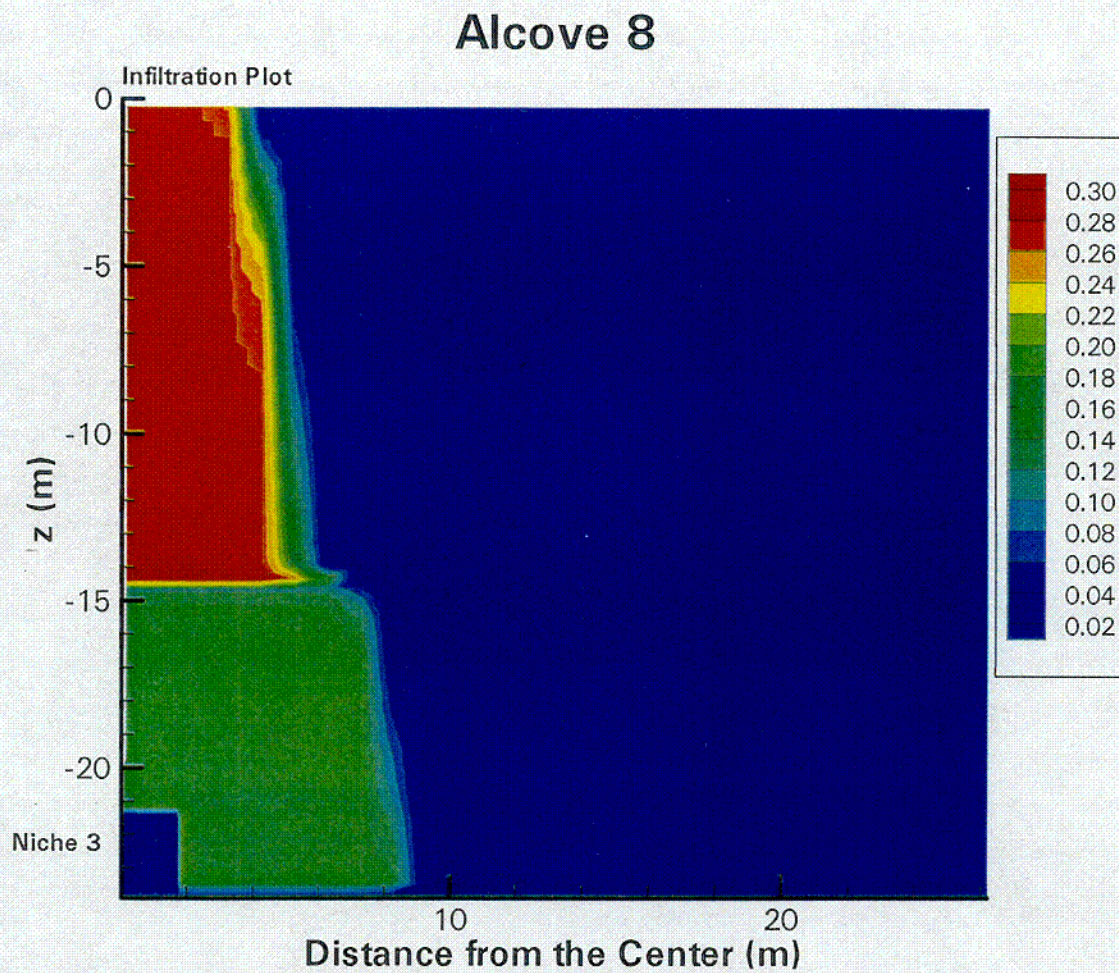


Figure 10. Predicted Distribution of Matrix Saturation Increase at the End of the Test (1 year) and at 10 years for the Drift-Scale Property Set.

(a) $t = 1$ year



(b) $t = 10$ years

Alcove 8

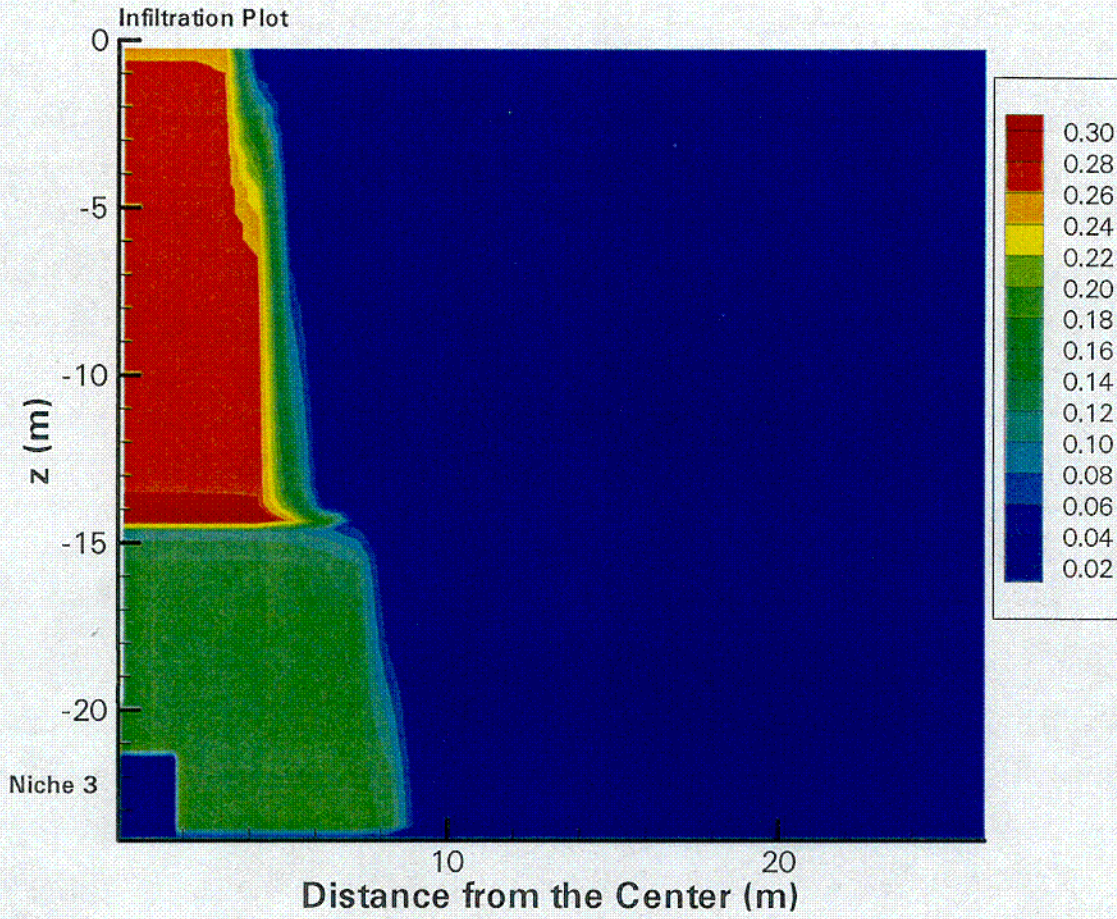
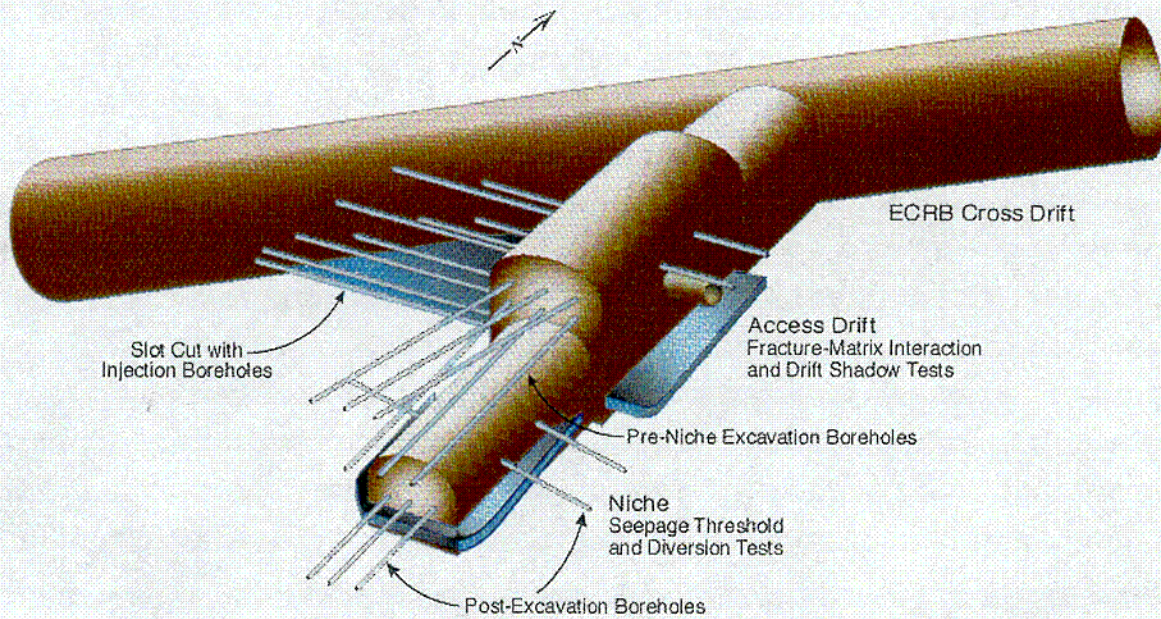


Figure 11. Niche 5 test site with horizontal and slanted boreholes above the niche ceiling for seepage threshold testing, lateral boreholes, and slot for wetting-front detection and seepage-diversion testing, and test bed for fracture-matrix interaction testing.



7701-002

Figure 12. Predicted Breakthrough Curves at Niche 3 for the Large Plot Test Using Three Property Sets. Relative Concentration Refers to the Tracer Concentration Collected at Niche 3 Divided by the Tracer Concentration at the Infiltration Plot. Solid and Dashed Lines Correspond to Br and PFBA, respectively.

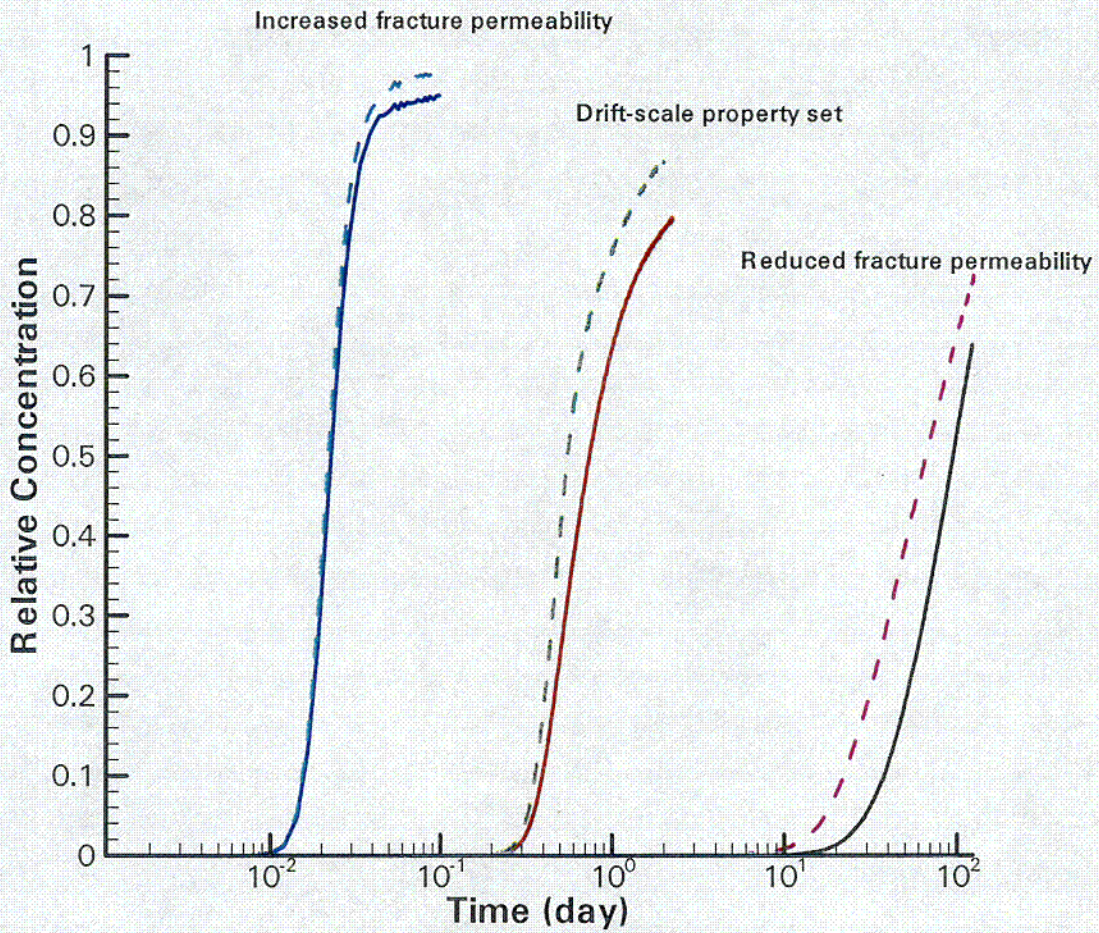
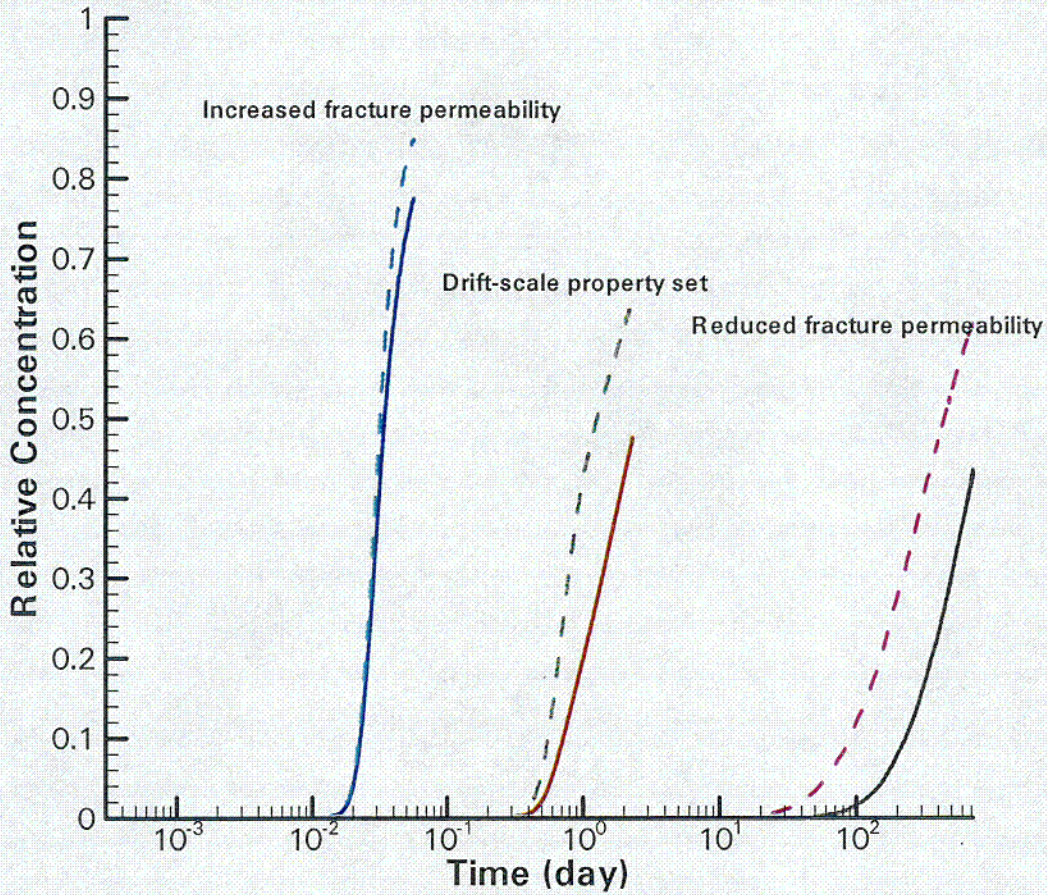


Figure 13. Predicted Breakthrough Curves at Niche 3 for the Small Plot Test Using Three Property Sets. Relative Concentration Refers to the Tracer Concentration Collected at Niche 3 Divided by the Tracer Concentration at the Infiltration Plot. Solid and Dashed Lines Correspond to Br and PFBA, respectively.



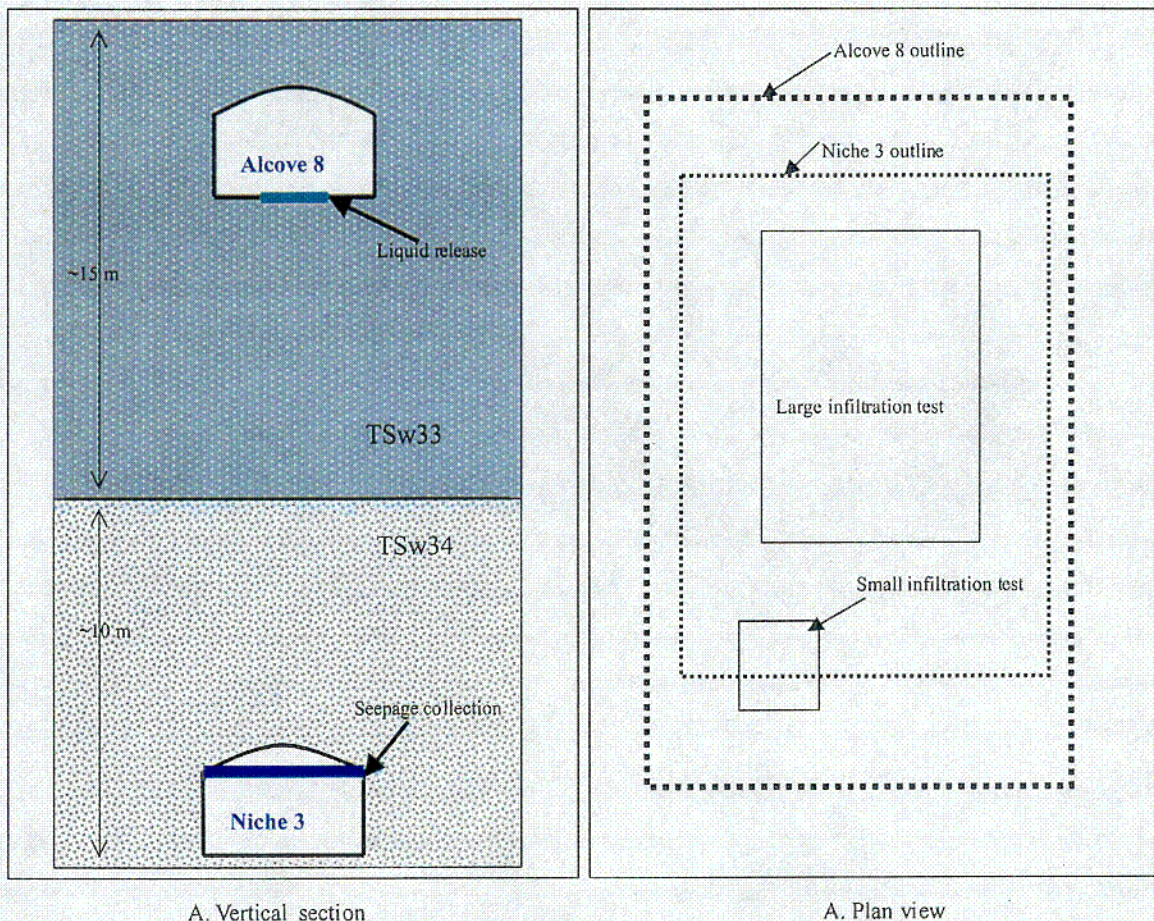
Attachment I
Alcove 8-Niche 3 Cross-Over Test Plan Revision 01

Objectives

The cross-over test is located at the unique location where Alcove 8 in the Enhanced Characterization of Repository Block (ECRB) Cross Drift is ~ 20 m directly above Niche 3 in the Exploratory Studies Facility (ESF) Main Drift, as illustrated in Figure I-1. In the cross-over test, liquid releases from Alcove 8 are detected at Niche 3. The test objectives are:

- Quantify large-scale (~ 20 m) infiltration and seepage processes in the potential repository horizon.
- Evaluate matrix imbibition and tracer diffusion mechanisms in long-term tests.
- Characterize fault and fractures across a lithophysal-nonlithophysal interface.
- Evaluate fracture-matrix interaction and estimate fracture-matrix interface area by analysis and modeling of tracer test results.

Figure I-1. Layout of Alcove 8 - Niche 3 Cross-Over Test Bed.



Test Plan Development

Following Alcove 1 test near the ground surface, the cross-over test plan was formulated during the ECRB Cross Drift design and excavation period for the excavation of a new Alcove 8 over the existing Niche 3 for a similar large-scale test in the potential repository horizon. Controlled liquid-release tests with tracers were planned with different phases. The original plan before Alcove 8 excavation was to start with infiltrimeter tests on a bench excavated at the Alcove 8 end wall, directly located above the ESF Main Drift. The test results were planned for use in the Determination of Importance Evaluation and for tracer-permit application. The bench after excavation did not intersect major fractures, and the bench test was relocated to a small plot on the floor along a fault. The fault, observed after Alcove 8 excavation as illustrated in Figure I-2, is located directly above the existing bulkhead of Niche 3. The small-plot test was conducted in year 2000. The small-plot tests are followed by line-release (~ 5 m long) tests along the fault in early 2001, and by a large 3 m × 4 m plot for areal release tests, as illustrated in Figure I-3.

Figure I-2. Location of the Fault along Alcove 8 Floor, Showing the Small Plot for Liquid Release into a 1 m Long Fault Trace.

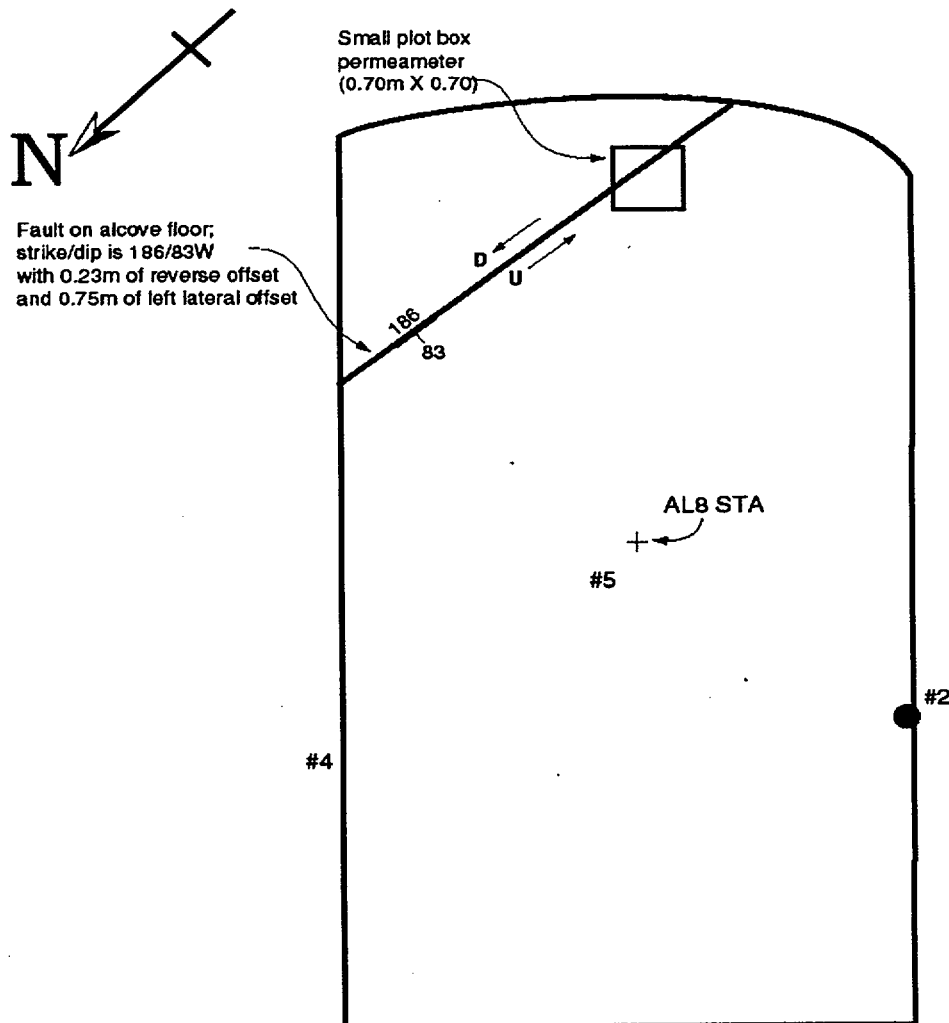
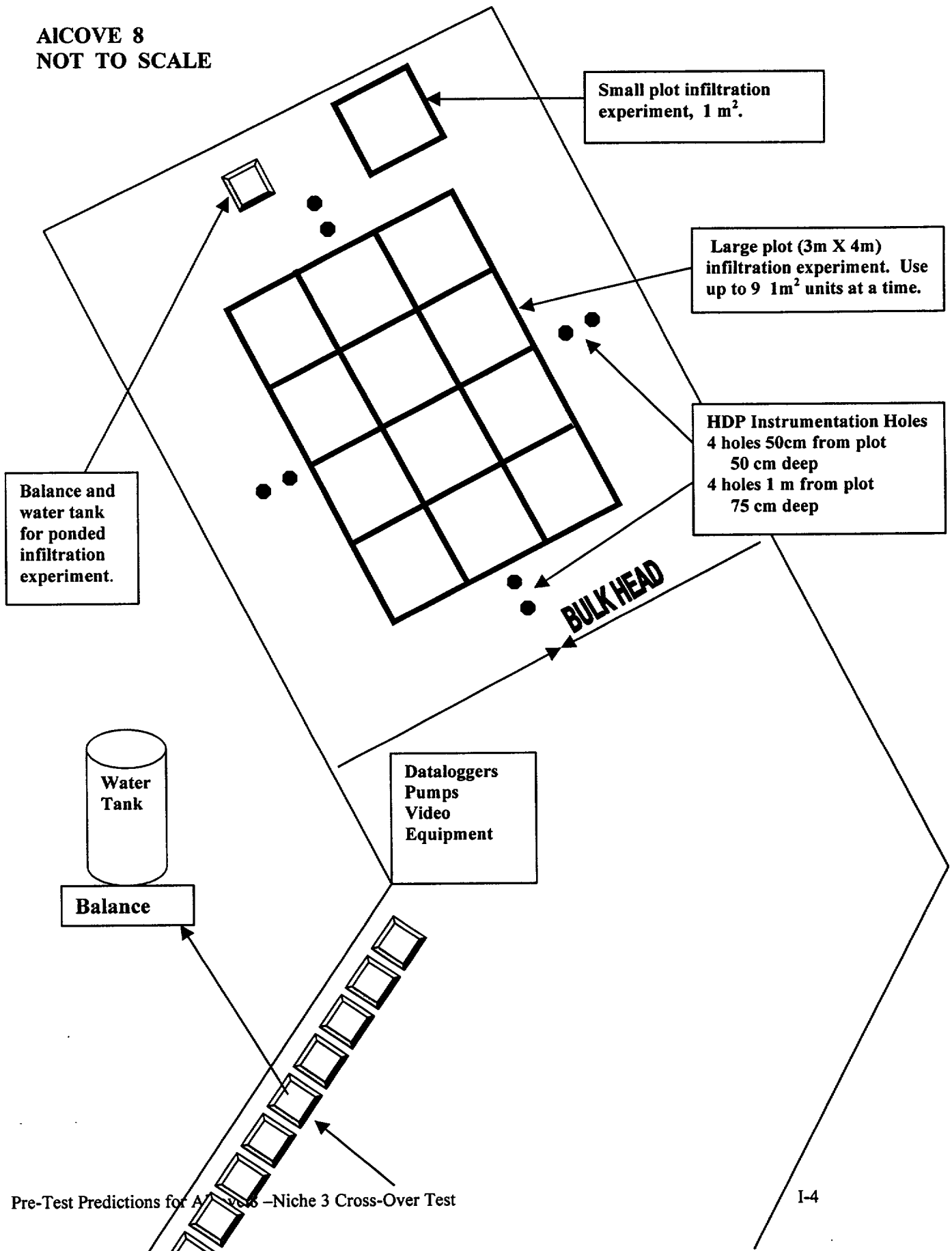


Figure I-3. Alcove 8 Infiltration.

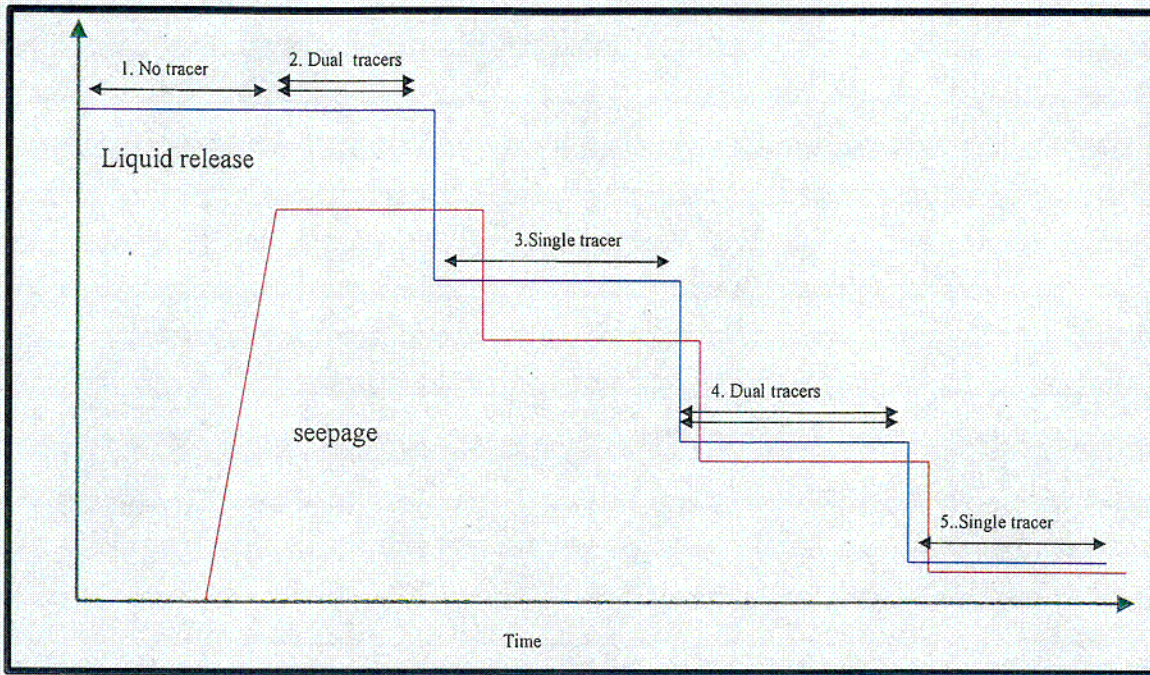
AICOVE 8
NOT TO SCALE



Approaches

Both active testing and passive monitoring programs are used to measure induced seepage at Niche 3 from controlled liquid releases at Alcove 8.

- Water releases are in Alcove 8 from a small plot along a fault, along the full length of the fault, and later from a large 3 m × 4 m plot, as illustrated in Figures I-2 and I-3.
- Alcove 8 is instrumented with heat dissipation probes (HDP) for potential measurements (Figure I-3).
- Geophysical measurements (neutron logging and ground penetrating radar) and cross-hole air-injection tests are conducted in vertically slanted boreholes, as illustrated in Figure I-4.
- Niche 3 is instrumented with wetting-front sensors (electrical resistivity probes) in boreholes (Figure I-5) and seepage collector. (Figure I-6 is for the fault test, with fault trace observed both inside and outside the bulkhead of Niche 3. Figure I-7 is for the large-plot test with collectors covering the whole niche).
- Slots along the Niche 3 walls may be considered to supplement the seepage collectors.
- Liquid release rate under constant head or constant tension test conditions, together with geophysical imaging and wetting-front detection, is used to characterize drainage.
- Fractures and features on the floor of Alcove 8 and ceiling of Niche 3, together with borehole logs, are mapped to correlate with the flow path observations.
- Evaporation rate and relative humidity conditions behind bulkhead are monitored to estimate the correction factor for seepage rate. Figure I-8 illustrates an automated evaporation measurement equipment for comparative measurements inside the niche and immediately outside the niche close to the bulkhead. The water level in an evaporation pan is maintained by a reservoir with pressure transducers to measure water loss.
- Multiple tracers with different diffusivity values are used in a series of liquid-release tests, broadly outlined in the following sequence.



Proposed sequence of tests in Alcove 8-Niche 3 Cross-over Test.

Figure I-4. Boreholes between Alcove 8 and Niche 3.

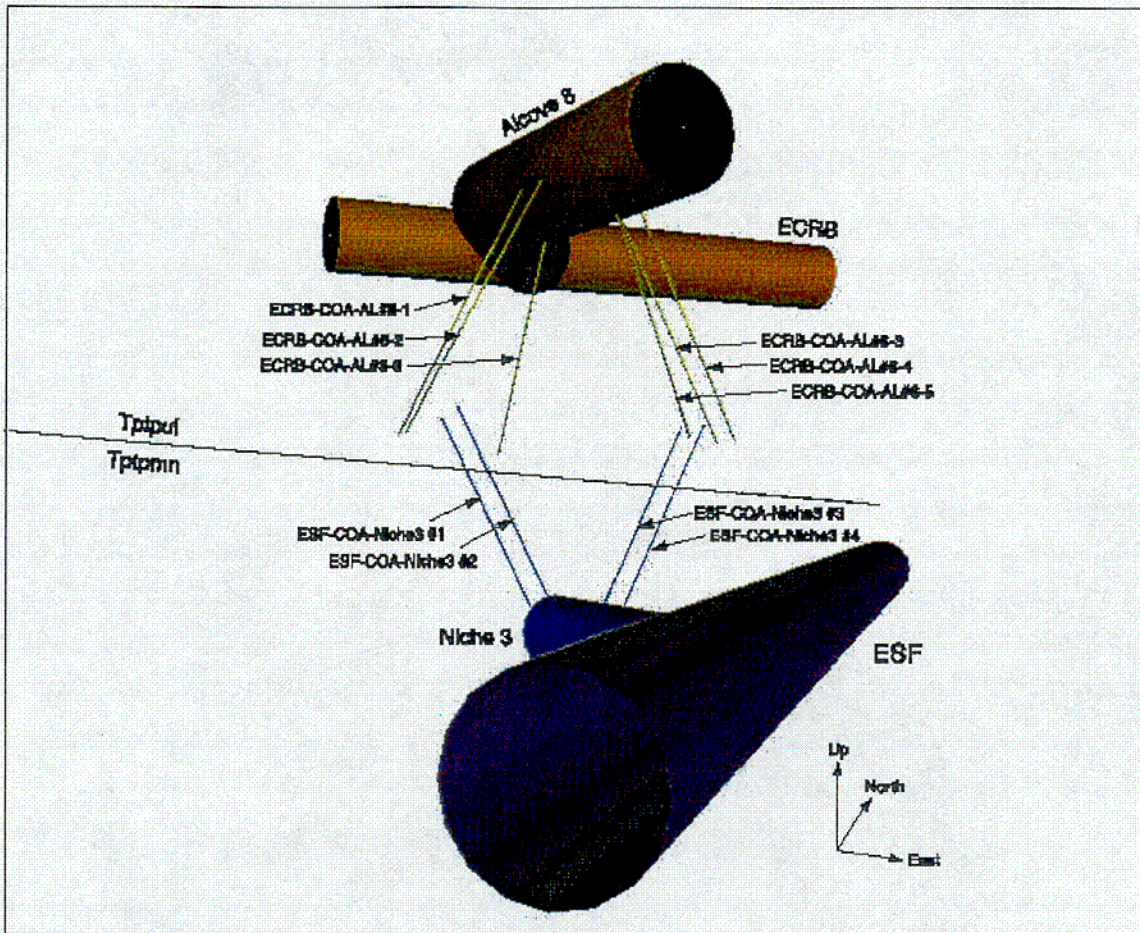
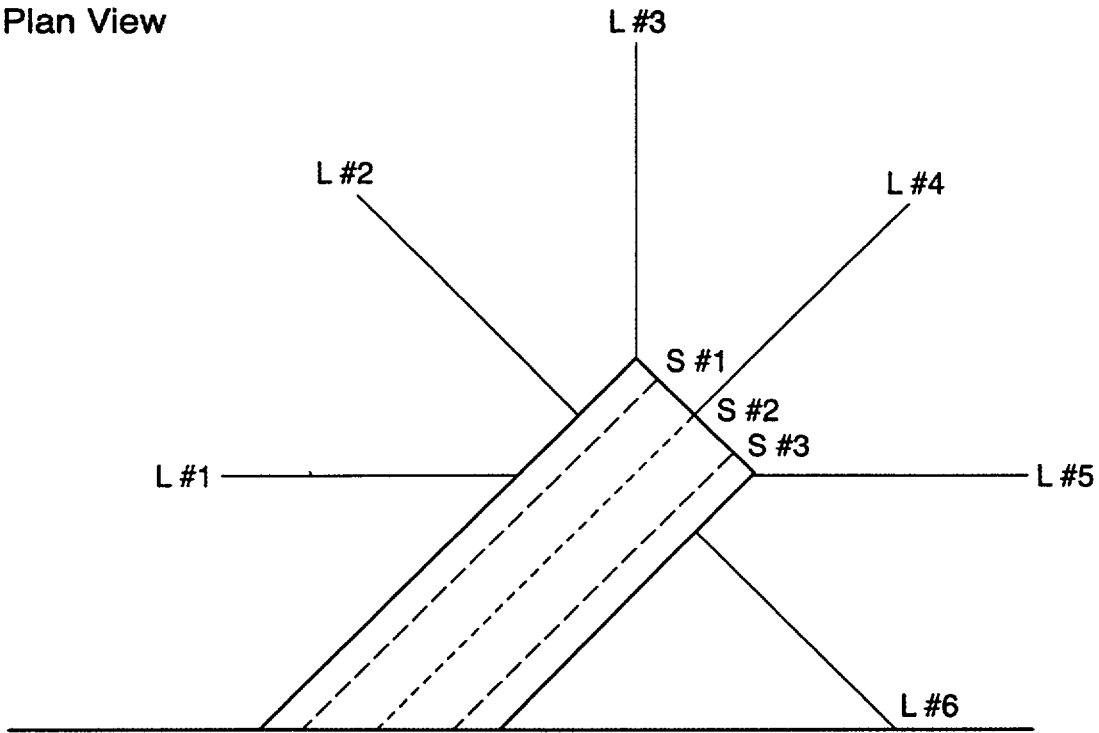
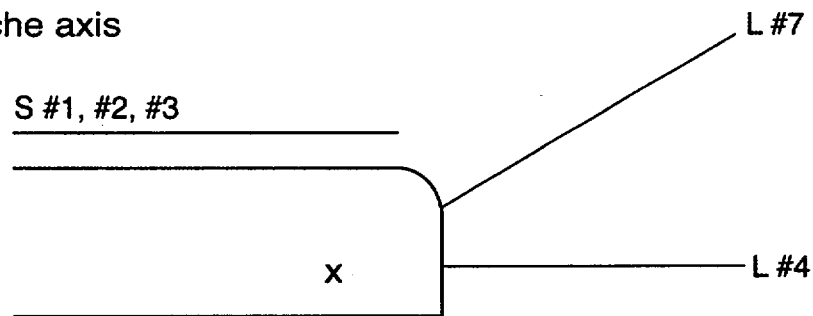


Figure I-5. Boreholes with Wetting Front Detectors (Electrical Resistance Probes) in Niche 3.

Plan View



Vertical Cross-section along Niche axis



0 2 4 Meters

AT2K010

Figure I-6. Seepage Collection System Installed near the Bulkhead in Niche 3 for the Fault Test.

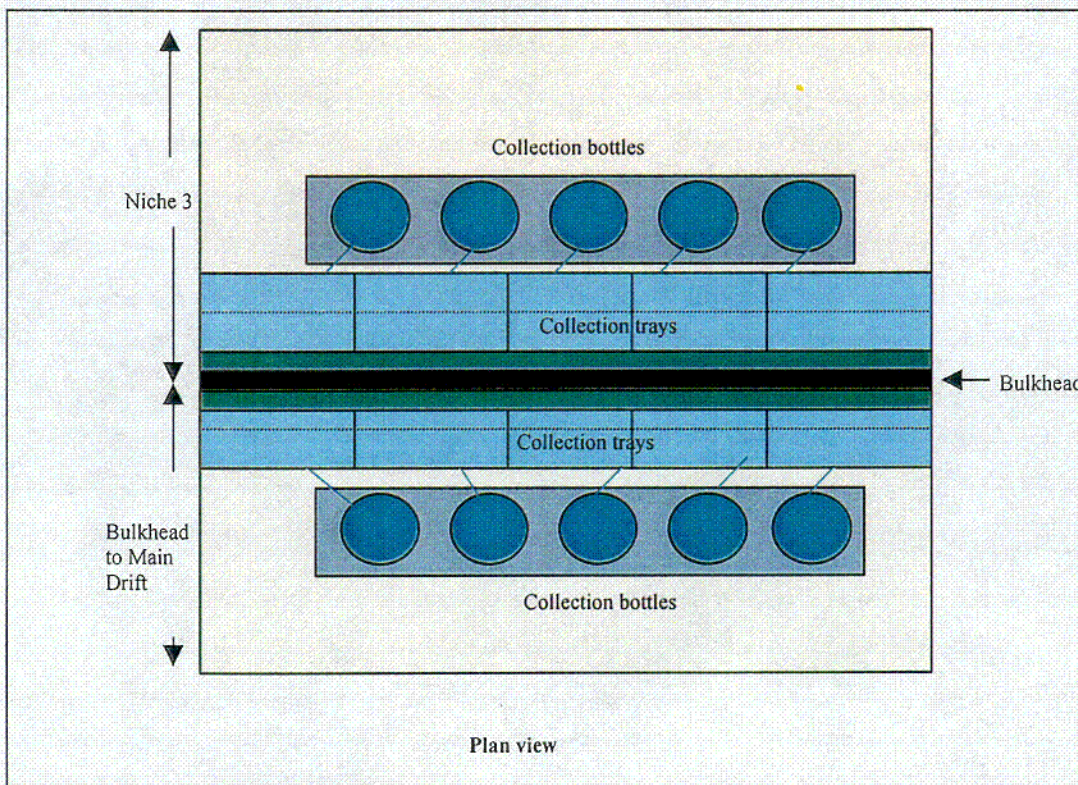
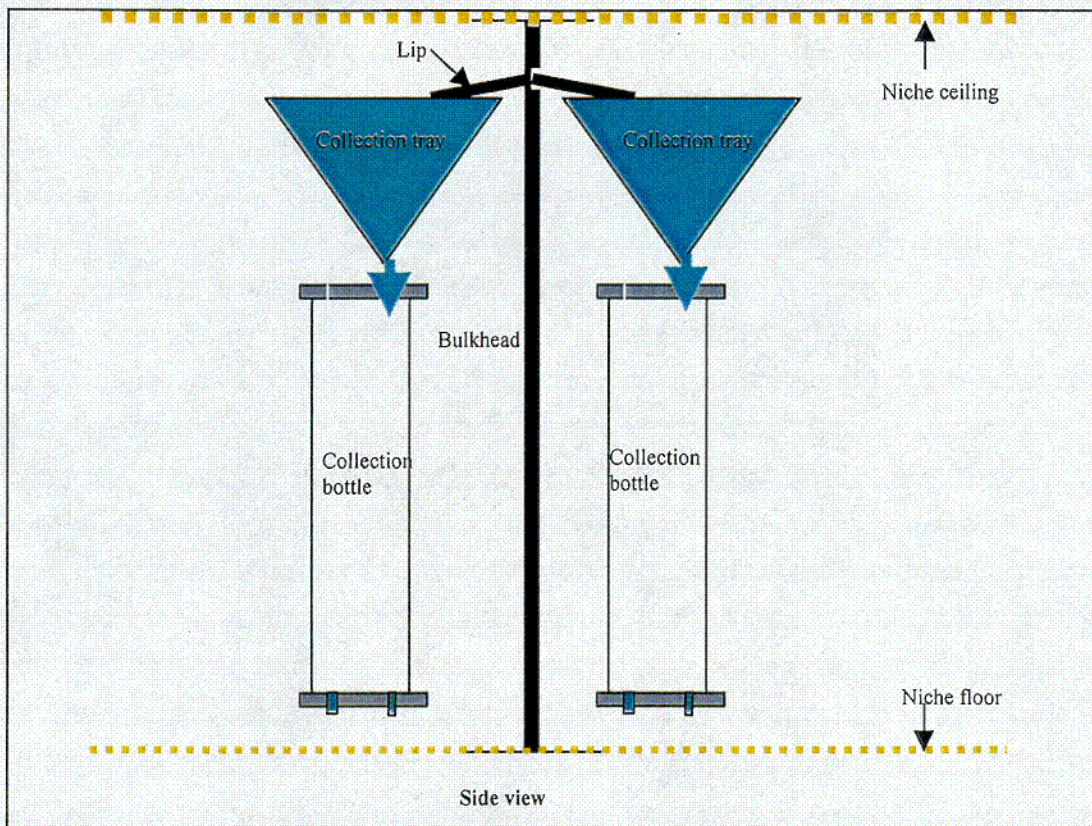


Figure I-7. Seepage Collection System for the Large-Plot Tests with Niche 3 Areally Covered with Existing Seepage Grid inside the Niche, Odd-Shaped Grids Behind and Before the Bulkhead, and Rectangular Grid in the ESF Main Drift.

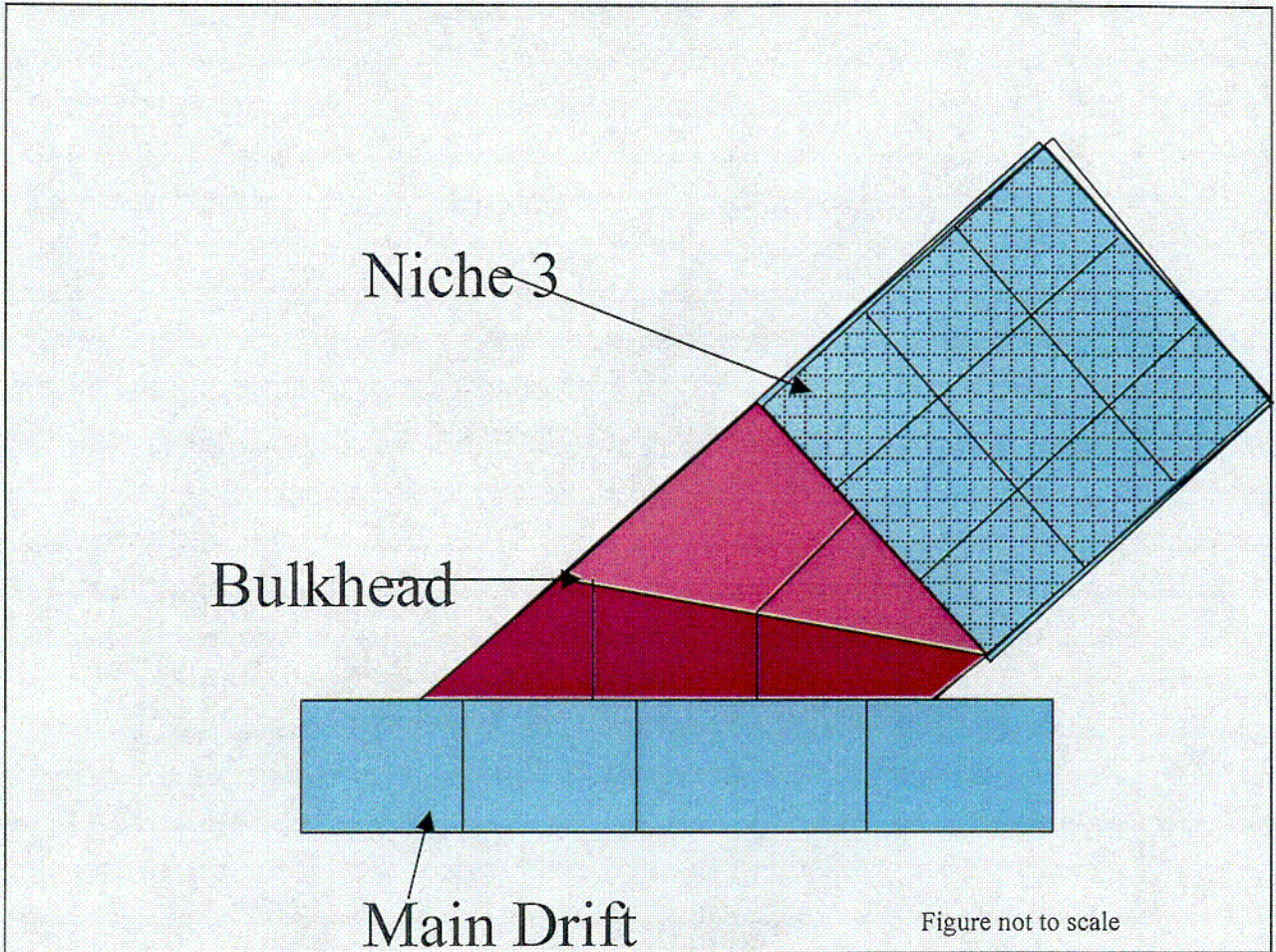
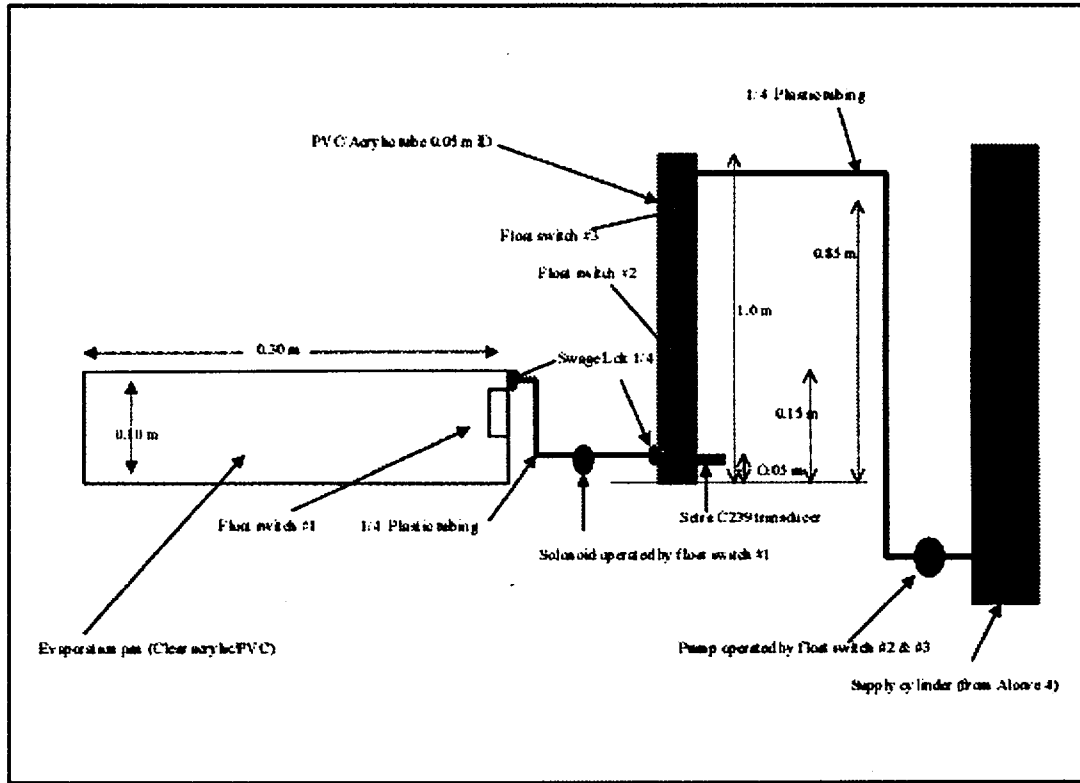


Figure I-8. Automated Evaporation Measurement Equipment for Comparative Measurements Inside the Niche and Immediately Outside the Niche Close to the Bulkhead.



Reh & Saha #3100

Both the fault test sequences and the large block tests will consider combinations of the following test components.

Phase I. Saturated Flow and Transport

1. Start the test with constant head (~ 2 cm water) until near-steady seepage is observed in Niche 3.
2. Introduce two tracers with different molecular diffusion coefficients (Br and PFBA) into the release water with the same boundary condition (constant water head).

The Phase I test will provide information on:

- a. *Importance of matrix diffusion (by analyzing the tracer breakthrough curves).*
- b. *Saturated hydraulic conductivity for fractures based on observed liquid release fluxes at Alcove 8.*
- c. *Fracture porosity by analyzing tracer test results for PFBA (which has a smaller molecular diffusion coefficient).*
- d. *Fracture-matrix interface area under saturated conditions by matching the tracer test results (if matrix diffusion is important)*

Phase II. Unsaturated Flow and Transport

3. Reduce the flux or apply negative pressure (tension) at upper boundary. Add a new single tracer after a near-steady seepage rate is observed in Niche 3.
4. Repeat Step 3 for a few tests with lower fluxes or more tension. Two tracers will be used for at least one test in Phase II.

The Phase II test will provide information on:

- e. *Fracture-matrix interface area as a function of flux by analyzing tracer test results for different infiltration fluxes.*
- f. *Flow and transport properties using iTOUGH2 for calibration.*
- g. *Fracture relative permeability as a function of flux.*

Additional Tests

The series of tests from high to low fluxes or increasing tensions can be followed by tests with a reversed order. There is no major basic and practical difference between descending and ascending sequences. In general, higher rate tests can reach near-steady states faster and induce shorter water-contact times with the rock matrix along the flow paths. A test with long duration will require a long recovery period for the formation to return to near-ambient conditions. The models developed for the tests will take into account the memory effects between tests with different rates and different rest periods. General approaches are adopted and specific details are evaluated on a test-by-test basis. This modeling-testing approach will be used for further refinements of the test series and for future deployment of larger-scale tests.

Time Frame

Once near-steady seepage has occurred in Niche 3, a series of tracer tests with different flux rates will be conducted. The first test can be used to estimate the duration of subsequent tests. A total of approximately four different fluxes rates will be used.

The test duration depends on the hydrological properties that are spatially variable. During and after the tests, numerical modeling will be performed to analyze and interpret observations and predict the test conditions. Data analysis and model interpretation can be used to determine if test duration is sufficient and flow rate and tracers can be changed.

Tracers and Analysis

Below is a list of tracers proposed for the test. Note that there are more tracers than those that can be used for the five tests to indicate that tracers are available if more than five tests are conducted.

Table I-1. Tracer Application Design at Alcove 8-Niche 3

Tracer Phase	Tracer Chemical	Aqueous Diffusion Coefficient ($m^2/s \times 10^{-10}$)
Release 2	LiBr + PFBA	Br ⁻ : 20.8; PFBA: 7.6
Release 3	2,4-DFBA	8.1
Release 4	Iodide + 2,6-DFBA	I ⁻ : 20.5; 2,6-DFBA: 8.1
Release 5	2,3,4,5-TeFBA	7.8
	2,5-DFBA	8.1
	3,4,5-TFBA	7.9
	2,4,5-TFBA	7.9
	2,4,6-TFBA	7.9

Abbreviation:

PFBA: pentafluorobenzoic acid
TEFBA: tetrafluorobenzoic acid
TFBA: trifluorobenzoic acid
DFBA: difluorobenzoic acid

The use of fluorinated benzoic acids (FBAs) as water tracers has received considerable attention, because FBAs are generally nonreactive, resistant to degradation, and relatively easy to be analyzed. The choice of sixteen derivatives of FBA tracers is especially useful for studies that require multiple nonreactive tracers. Furthermore, FBA tracers have larger molecular sizes than the halide tracers, which could be exploited to investigate the

contribution of diffusive mass transfer (e.g., matrix diffusion) to solute transport. The application of FBAs is pending on the use permit under review.

Test Participation

The USGS is responsible for infiltration and heat dissipation probe (HDP) (and other potential instrumentation) installation in Alcove 8, and neutron logging in boreholes.

LBL is responsible for the seepage sample collection and wetting-front detection in Niche 3, tracer analysis, crosshole air injections, ground-penetrating-radar tomography studies from boreholes, data analyses and model calibration with UZ flow, transport and seepage models.

Attachment II
Modeling Predictions for Flow in the Small Plot Test

Introduction

Relevant test prediction modeling results for the small-plot tests associated with a nearly vertical fault are presented to assess the efficiency of cutting slots along the wall of Niche 3 for water-diversion estimates. A sensitivity study was performed to identify key rock properties that would determine the experimental observations. Infiltrometer data from the ECRB Cross Drift benches were used for the relative permeability functions. The model prediction, calibration, and verification methodology to be used in the Alcove 8-Niche 3 tests are the same approaches used in other seepage and flow test locations in the ESF drifts. For Alcove 8-Niche 3, additional modeling for larger-scale tests are on-going and will be reported in the Unsaturated Zone Process Model Report and associated Analysis/Model Reports.

Model

For the small-plot test, a water-pressure head of 2 cm has been kept on the alcove floor during the test, and wetting-front arrival time and seepage are monitored at Niche 3. The nearly vertical fault was represented by a single fracture, and a two-dimensional, vertical model was developed to simulate the small-plot test. On each side of the vertical fracture, matrix thickness is determined by average fracture spacing. Fracture apertures were determined from the fracture porosity data. To capture the transient behavior for flow between the fault and the matrix, a multiple interacting continua grid with five matrix continua was employed.

The drift-scale property set (Table II-1) was used in the modeling study. Fracture permeability values measured with disk infiltrometer are consistent with the drift-scale fracture permeability values in Table II-1. A new combination of van Genuchten capillary-saturation relation and a modified Brooks-Corey relative permeability-saturation relation was used as fracture constitutive relations, as illustrated in Figure II-1. Details of characteristic curve fitting are to be documented in an Analysis/Model Report.

Figure II-1. Fit of the Brooks-Corey Relative Permeability-Capillary Pressure Relation to the Measured Data.

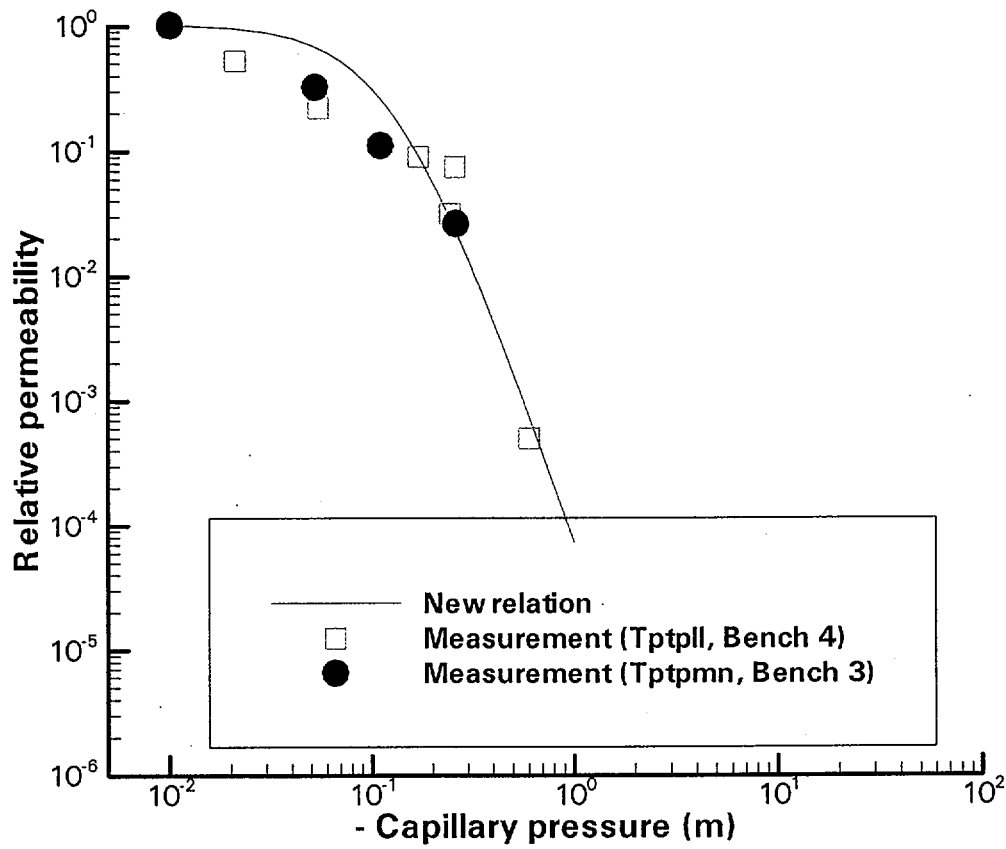


Table II-1. Rock Properties Used in the Model Prediction

Rock property	TSw33		TSw34	
	Fracture	Matrix	Fracture	Matrix
Permeability (m ²)	5.5E-13	3.08E-17	2.76E-13	4.07E-18
Porosity	6.6E-3	0.154	1.E-2	0.11
Fracture spacing (m)	1.23		0.23	
Fracture aperture (m)	1.49E-3		7.39E-4	
van Genuchten alpha (Pa ⁻¹)	1.46E-3 1.00E-3 ^a	2.13E-5	5.16E-4 1.00E-3 ^a	3.86E-6
van Genuchten m	0.608 0.458 ^a	0.298	0.608 0.458 ^a	0.291
Residual saturation	0.01	0.12	0.01	0.19
Initial saturation	1.05E-2	0.72	1.05E-2	0.85

^a Alternative van Genuchten parameters fitted to infiltrometer data.

Results of Sensitivity Study and Prediction

A sensitivity study was performed to evaluate effects of parameter uncertainty on model prediction. The selected parameter (for both TSw34 and TSw33) was varied from (while other parameters are the same as) those given in the drift-scale parameter set. The recoverability is most sensitive to fracture permeability, as illustrated in Figure II-2. The recoverability is defined as the total volume of water collected at Niche 3 divided by the total volume of water applied from the infiltration plot. The increased and reduced fracture permeabilities are given by $20K_f^*$ and $K_f^*/20$, respectively, where K_f^* is fracture permeability given in Table II-1. These values roughly correspond to $K_f^* \times 10^{2\sigma}$ and $K_f^* \times 10^{-2\sigma}$, respectively, where σ is the standard deviation of $\log(K_f)$ for TSw34.

Higher fracture permeability corresponds to an earlier wetting-front arrival time. The results of the sensitivity study for other parameters are summarized in Figure II-2. Fracture alpha generally has a relatively insignificant effect on the arrival time but a considerable effect on the recoverability, because a smaller fracture alpha gives rise to a stronger capillary barrier effect. The simulated results are also found to be insensitive to the fracture porosity, but quite sensitive to matrix permeability and matrix alpha.

Figure II-2. Model Prediction Results for Increased (x20) and Reduced (/20) Fracture Permeabilities from the Drift-Scale Property Set.

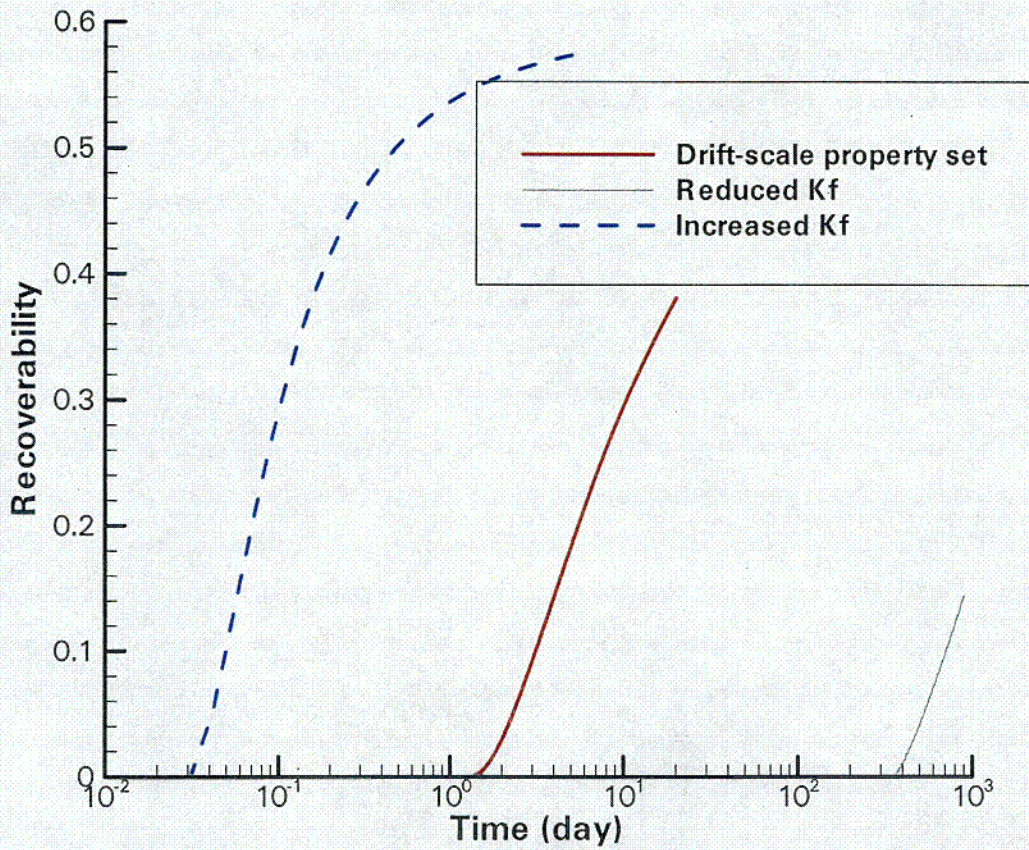


Figure II-3. Results of Sensitivity Study for (a) Different Fracture Capillarity Parameter Alpha, (b) Different Fracture Porosity, (c) Different Matrix Permeability (Km), and (d) Different Matrix Alpha.

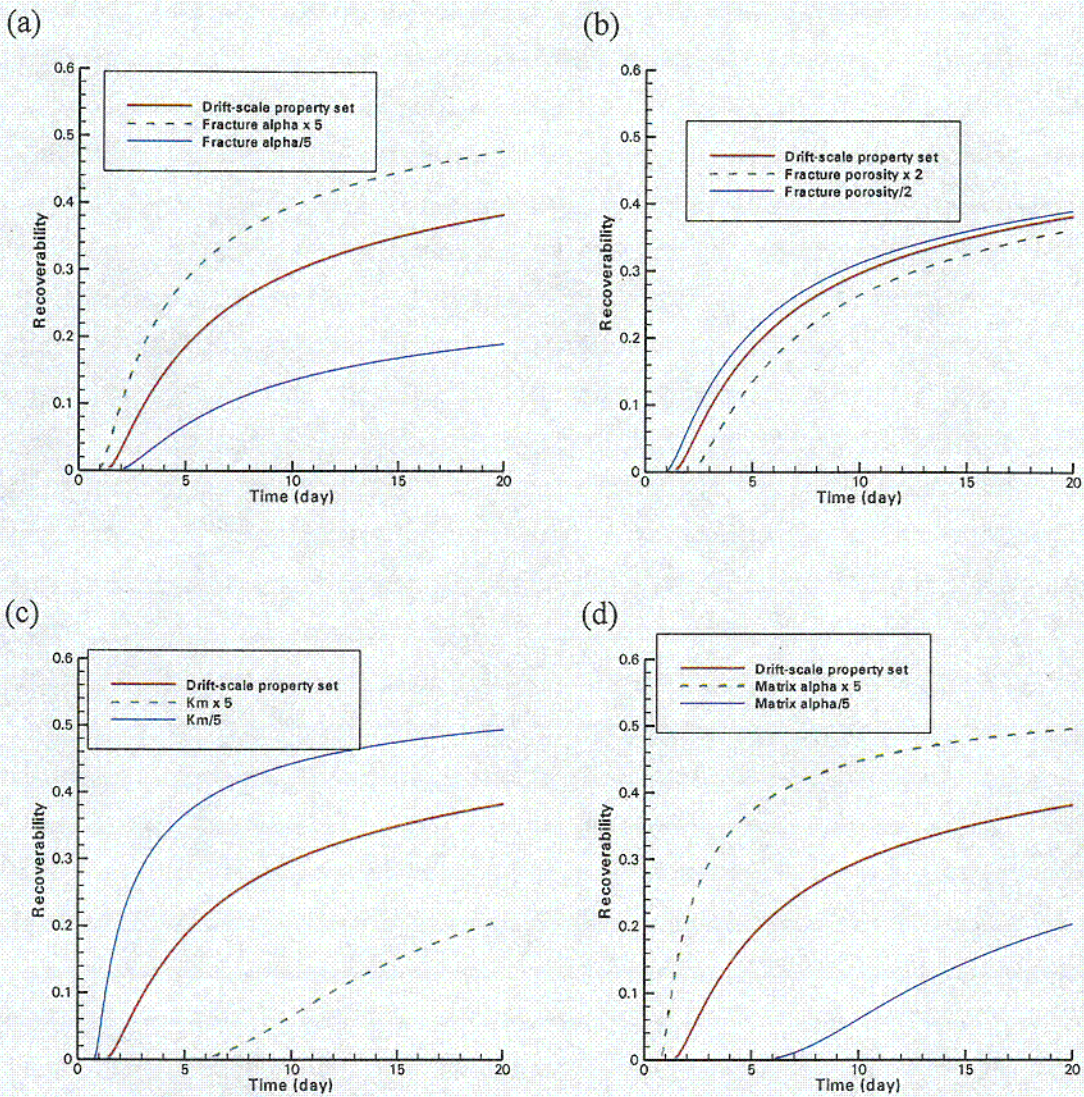
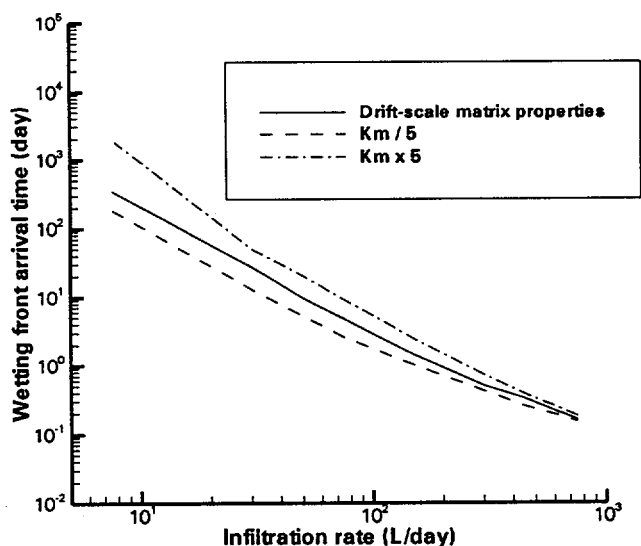


Figure II-4 summarizes simulated relations between the arrival time and infiltration rate from the small plot. The infiltration rate is approximately proportional to fracture permeability (representing the fault). Because the infiltration rate can be easily measured before the wetting front is observed at Niche 3, this figure is useful for *in situ* prediction of the arrival time based on the observed infiltration rate. If the infiltration rate is assumed to be 10 L/day, predicted arrival time is between 100 to 1,000 days, as shown in Figure II-4.

For each curve in Figure II-4, the rock property values are fixed except for fracture permeability (representing the fault). The fracture permeability of the fault is to be determined by the observed infiltration rate. There are large uncertainties associated with specific flow path properties. Similar uncertainties of predictive study were evaluated at the Alcove 1 infiltration test, with the first arrival of wetting front (in ~58 days) much longer than the subsequent capillary pressure responses (~2-3 days). The storage effects along the flow paths can greatly affect the arrival time. Once a flow path was wetted, the flow might be much faster. The flow path properties associated with the fault through the cross-over test bed in the potential repository horizon are unknown. The on-going small-plot and fault tests can elucidate the hydrological properties of the flow paths and establish the base for tracer tests for quantifying the transport properties after the flow field is established.

Figure II-4. Preliminary Simulated Relations between the Wetting-Front Arrival Time and the Infiltration Rate of the Small Plot. The solid curve corresponds to the drift-scale property set. Properties used for the other curves are the same as those used for the solid curve (except matrix permeability and alpha). Matrix alpha is related to matrix permeability with the Miller-Miller similarity.



Spatial Distributions of Flow

Length of test period depends on the infiltration rate (fracture permeability). Under the current test plan, the length is roughly 90 days and 3 years for the drift-scale property set and the reduced fracture permeabilities, respectively. Figure II-5 shows simulated distributions of matrix saturation increase at the end of the test and at $t = 10$ years. The matrix saturation increase is determined to be the difference between simulated matrix saturations with and without consideration of the test. Initially, matrix saturation is 0.72 and 0.85 for TSw33 and TSw34, respectively. These values are consistent with field observation reported. Because centers of the infiltration plot and Niche 3 are different, the distributions are not symmetric. These results suggest that the test hardly affects rock hydrologic conditions for a location about 20 m away from the niche center (in the horizontal direction). The model domain may need to be extended below the niche to eliminate any boundary effects.

Figure II-5. Predicted Distributions of Matrix Saturation at Different Times with Different Fracture Permeability: (a) Drift-Scale Property Set at 90 Days, (b) at 10 Years, (c) Reduced Permeability at 3 Years, and (d) at 10 Years.

